Chapter 5
Examples of Thermokinetic Investigations

5.1 Isothermal, Discontinuous, Constant-Volume Reactions

5.1.1 Reaction of a Sulphide with Hydrogen Peroxide

As an example of the elaboration of a kinetics on the basis of

- Data of non-isothermal, discontinuous reactions
- Mathematical-analytical relations

the catalytic consecutive reaction of a substituted sulphide with hydrogen peroxide to sulpho acid is discussed:

$$R_1 - S - R_2 + 3H_2O_2 \rightarrow R_1^{'} - R_2^{'} - SO_3H - R_3^{'}.$$

The process takes place in three stages:
(1) from sulphide to sulphoxid, (2) to sulphone (3) to sulpho acid:

$$R_1 - S - R_2 \xrightarrow[H_2O_2,\,Cat]{r_1,\,\Delta H_1} R_1 - SO - R_2 \xrightarrow[H_2O_2,\,Cat]{r_2,\,\Delta H_2}$$
$$R_1 - SO_2 - R_2 \xrightarrow[H_2O_2,\,Cat]{r_3,\,\Delta H_3} R_1^{'} - R_2^{'} - SO_3H - R_3^{'}.$$

W. Litz, *Bench Scale Calorimetry in Chemical Reaction Kinetics*,
DOI 10.1007/978-3-319-12532-9_5

The stoichiometric coefficients are

$$\begin{aligned} &\nu_{\mathrm{R1-S-R2,1}} = -1, \nu_{\mathrm{H2O2,1}} = -1, \nu_{\mathrm{R1-SO-R2,1}} = 1, \nu_{\mathrm{R1-SO2-R2,1}} = 0, \\ &\qquad \nu_{\mathrm{R'1-R'2-SO3H-R'3,1}} = 0, \\ &\nu_{\mathrm{R1-S-R2,2}} = 0, \nu_{\mathrm{H2O2,2}} = -1, \nu_{\mathrm{R1-SO-R2,2}} = -1, \nu_{\mathrm{R1-SO2-R2,2}} = 1, \\ &\qquad \nu_{\mathrm{R'1-R'2-SO3H-R'3,2}} = 0, \\ &\nu_{\mathrm{R1-S-R2,3}} = 0, \nu_{\mathrm{H2O2,3}} = -1, \nu_{\mathrm{R1-SO-R2,3}} = 0, \nu_{\mathrm{R1-SO2-R2,3}} = -1, \\ &\qquad \nu_{\mathrm{R'1-R'2-SO3H-R'3,3}} = 1. \end{aligned} \tag{5.1}$$

It is known that acids (such as sulphuric acid, nitric acid) catalyse the first stage; the second and third stages require additionally the use of potassium permanganate or sodium molybdate as catalyst.

To conduct the kinetic investigation, the measuring kettle of the calorimeter is filled with a batch of sulphide, Na_2MoO_4, H_2O_2 and xylene because the industrial production is run under conditions of cooling by reflux. The batch is brought to reaction temperature and H_2O_2 is injected simultaneously at the start of the reaction.

Figure 5.1 shows, for $T = 50$ °C, the temporal course of the caloric reaction power after instantaneous addition of different amounts of H_2O_2 (50 %).

The conversion has the following appearance

- The characteristic course of the thermal reaction power is independent of the amount of the abruptly injected H_2O_2:
  after a certain time t_E of uniform decay, the caloric reaction power decreases relatively abruptly and in a short time interval reaches the value zero;
- The time t_E increases by the increased addition of H_2O_2;
- The typical reaction does not change by increasing the concentration by the reduction of the aqueous part in the batch;

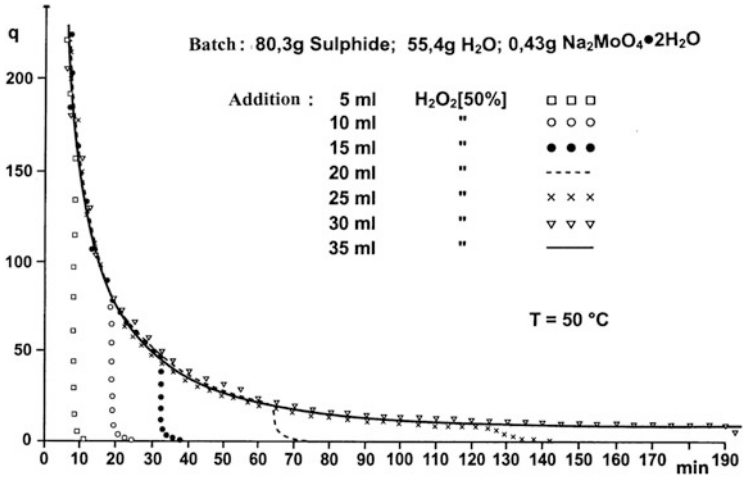

Fig. 5.1 Course of thermal reaction power q during oxidation of sulphide (95.5 % purity) for different amounts of dosed H_2O_2 (50 % purity)

- But the thermal reaction power increases; in contrast, the time interval up to the beginning of the almost abrupt decay of the rate of heat release diminishes.
- By the additional dose of H_2O_2 the phenomenon recurs, i.e. the thermal reaction power continues until it stops abruptly again after a time interval.
- When the added amount of H_2O_2 exceeds the stoichiometric amount for the total oxidation of the reaction system, the thermal reaction power no longer stops abruptly but decreases gradually to zero.
- When the first dosed amount of H_2O_2 exceeds the amount necessary for complete oxidation, the thermal reaction power diminishes, right away monotonously, to zero.
- The oxidation of sulphoxid or sulphon shows the same characteristic behaviour.

Obviously, the reaction steps are not elementary reactions, because the caloric reaction power respectively rate of reaction depends only on the concentration of sulphide, sulphoxid or sulphon but does not depend on the concentration of the reactant H_2O_2. Such a phenomenon occurs under special conditions when the catalyst first reacts reversibly with one of the reactants (Michaelis Menton mechanism); in the present case:

$$\mathrm{A} + \mathrm{Cat} \underset{r_2', \Delta H_{\lambda 2}}{\overset{r_1', \Delta H_{\lambda 1}}{\rightleftharpoons}} \mathrm{A} \,\text{¤}\, \mathrm{Cat}$$

$$\mathrm{B} + \mathrm{A} \,\text{¤}\, \mathrm{Cat} \xrightarrow[r_3', \Delta H_{\lambda 3}]{} \mathrm{C} + \mathrm{Cat}$$

with

A : H_2O_2
B : sulphide, sulphoxid, sulphone
C : sulphoxid, sulphone, sulpho acid
Cat : sodium molybdate

Stoichiometric coefficients

$$\begin{aligned} &\nu_{A1} = -1, \nu_{Kat1} = -1, \nu_{A\,¤\,Cat1} = 1, \nu_{B1} = 0, \nu_{C1} = 0, \\ &\nu_{A2} = 1, \nu_{Kat2} = 1, \nu_{A\,¤\,Cat2} = -1, \nu_{B2} = 0, \nu_{C2} = 0, \\ &\nu_{A3} = 0, \nu_{Kat3} = 1, \nu_{A\,¤\,Cat3} = -1, \nu_{B3} = -1, \nu_{C3} = 1. \end{aligned}$$

The intermediate product A¤Cat represents a, so to speak, activated H_2O_2; obviously, only in this state is a reaction with B for the production of C possible, by which the catalyst Cat returns to replenish the complex A¤Cat by means of the reservoir of A.

On the assumption that both the achievement of equilibrium and the following reaction occur by elementary steps, for the rate of change in the intermediate product A¤Cat and the rate of formation in the oxidized product C we obtain, corresponding to (4.9) and (4.34),

$$\mathrm{d}c_{\mathrm{A}\,¤\,\mathrm{Cat}}/\mathrm{d}t = k_1^{'} \cdot c_{\mathrm{A}} \cdot c_{\mathrm{Cat}} - k_2^{'} \cdot c_{\mathrm{A}\,¤\,\mathrm{Cat}} - k_3^{'} \cdot c_{\mathrm{A}\,¤\,\mathrm{Cat}} \cdot c_{\mathrm{B}}$$
$$\mathrm{d}c_{\mathrm{C}}/\mathrm{d}t = k_3^{'} \cdot c_{\mathrm{A}\,¤\,\mathrm{Cat}} \cdot c_{\mathrm{B}}. \tag{5.2}$$

Because the catalyst and, consequently, the activated intermediate complex A¤Cat are present only in very small concentrations, naturally there is not much leeway for this to change, and after a short initial phase the following equation holds (Bodenstein hypothesis):

$$k_1^{'} \cdot c_{\mathrm{A}} \cdot c_{\mathrm{Cat}} - k_2^{'} \cdot c_{\mathrm{A}\,¤\,\mathrm{Cat}} - k_3^{'} \cdot c_{\mathrm{A}\,¤\,\mathrm{Cat}} \cdot c_{\mathrm{A}} = 0.$$

With the initial concentration of the catalyst c_{Cat_0} we obtain, according to the mol balance, $c_{\mathrm{Cat}} = c_{\mathrm{Cat}_0} - c_{\mathrm{A}\div\mathrm{Cat}}$,

$$c_{\mathrm{A}\,¤\,\mathrm{Cat}} = \left[k_1^{'} \cdot c_{\mathrm{A}} \cdot c_{\mathrm{Cat}_0}\right] \Big/ \left[k_2^{'} + k_3^{'} \cdot c_{\mathrm{B}} + k_1^{'} \cdot c_{\mathrm{Cat}}\right].$$

A¤Cat does not fall into a state of congestion after the initial phase. Therefore, the rate of formation in the oxidized product C, the rates of consumption in reactants A and B and the rate of circulation in the intermediate complex A¤Cat correspond to one another. According to (5.2) the following equation is valid:

$$-\mathrm{d}c_{\mathrm{A}}/\mathrm{d}t = -\mathrm{d}c_{\mathrm{B}}/\mathrm{d}t = \mathrm{d}c_{\mathrm{C}}/\mathrm{d}t$$
$$= k_3^{'} \cdot k_1^{'} \cdot c_{\mathrm{Cat}_0} \cdot c_{\mathrm{A}} \cdot c_{\mathrm{B}} \Big/ \left[k_2^{'} + k_3^{'} \cdot c_{\mathrm{B}} + k_1^{'} \cdot c_{\mathrm{A}}\right]. \tag{5.3}$$

If the conversion velocity of reactant B with the intermediate complex A¤Cat is essentially smaller than the velocity at which chemical equilibrium is achieved between A, Cat and A¤Cat, i.e. $k_3^{'} \ll k_2^{'} < k_1^{'}$, (5.3) changes to

$$-\mathrm{d}c_{\mathrm{A}}/\mathrm{d}t = -\mathrm{d}c_{\mathrm{B}}/\mathrm{d}t = \mathrm{d}c_{\mathrm{C}}/\mathrm{d}t = k_3^{'} \cdot c_{\mathrm{Cat}_0} \cdot c_{\mathrm{B}} \cdot \gamma$$

with

$$\gamma = k_1^{'}/k_2^{'} \cdot c_{\mathrm{A}} \Big/ \left[1 + k_1^{'}/k_2^{'} \cdot c_{\mathrm{A}}\right].$$

The factor γ is a function of c_{A}. γ sets the tone for the temporal course of the overall rate. Within the range of high concentration with $k_1^{'}/k_2^{'} \cdot c_{\mathrm{A}} \gg 1$ the factor γ is constant, i.e. $\cong 1$. The intermediate complex A¤Cat is present in the largest possible concentration ($\cong c_{\mathrm{Cat}_0}$). The reaction rate is only proportional to the concentration of B, and the reaction runs at a rate of order 1:

$$-\mathrm{d}c_{\mathrm{A}}/\mathrm{d}t = -\mathrm{d}c_{\mathrm{B}}/\mathrm{d}t = \mathrm{d}c_{\mathrm{C}}/\mathrm{d}t \cong \left[k_3^{'} \cdot c_{\mathrm{Cat}_0}\right] \cdot c_{\mathrm{B}} = k\{c_{\mathrm{Cat}_0}\} \cdot c_{\mathrm{B}} = r. \tag{5.4}$$

If the concentration of A during the conversion decreases to the range of small concentration with $k_1^{'}/k_2^{'} \cdot c_A \ll 1$, then the factor γ holds:

$$\gamma \cong k_1^{'}/k_2^{'} \cdot c_A.$$

The intermediate complex $A \div Cat$ is not present now in practically unchanged concentration ($\cong c_{Cat_0}$) but changes directly proportionally to c_A. We obtain the following results:

$$\begin{aligned} -dc_A/dt = -dc_B/dt = dc_C/dt &= \left(k_3^{'} \cdot k_1^{'}/k_2^{'}\right) \cdot c_{Cat_0} \cdot c_B \cdot c_A \\ &= k\{c_{Cat_0}\} \cdot c_A \cdot c_B. \end{aligned} \tag{5.5}$$

The transition from the range with $\gamma \cong 1$, i.e. (5.4), to a range with $\gamma \cong k_1^{'}/k_2^{'} \cdot c_A$, i.e. (5.5), takes place more abruptly depending on the relation $k_1^{'}/k_2^{'}$, i.e. the larger the thermodynamic equilibrium constant of the equilibrium between A, Cat and $A \div Cat$, the more abrupt the transition.[1]

The course of the measured thermal reaction power versus time shows this occurrence in the form of a suddenly starting decay at t_{E1}, already reaching after a short time virtually the value zero at t_{E2} (Fig. 5.1). Hence, the transition of the reaction rate from (5.4) to (5.5) occurs immediately before the complete consumption of H_2O_2 at t_{E2}. Therefore, for simplification it is taken as a basis that the oxidation process runs according to the rate function (5.4) up to the complete conversion of H_2O_2 at the time t_E, for which the following expression holds: $t_{E1} < t_E < t_{E2}$, and t_E is determined according to $Q = \int_{t_{E1} \to t_{E2}} \left\{q_{(\text{measurement})}\right\} dt = \int_{t_{E1} \to t_E} \left\{q_{(\text{due to 5.4})}\right\} dt$.

The thermokinetic interpretation of the measured course of the thermal reaction power of the oxidation of sulphide via sulphoxid and sulphon up to sulpho acid is started on a trial basis according to the assumption of quasi-elementary steps, the stoichiometry and (5.1), (4.9), (4.34), with

$$dc_{R1-S-R2}/dt = -r_1 = k_1 \cdot c_{R1-S-R2}. \tag{5.6}$$

$$dc_{R1-SO-R2}/dt = r_1 - r_2 = k_1 \cdot c_{R1-S-R2} - k_2 \cdot c_{R1-SO-R2}. \tag{5.7}$$

$$dc_{R1-SO2-R2}/dt = r_2 - r_3 = k_2 \cdot c_{R1-SO-R2} - k_3 \cdot c_{R1-SO2-R2}. \tag{5.8}$$

$$dc_{R'1-R'2-SO3H-R'3}/dt = r_3 = k_3 \cdot c_{R1-SO2-R2}. \tag{5.9}$$

$$\begin{aligned} dc_{H2O2}/dt &= -r_1 - r_2 - r_3 \\ &= -k_1 \cdot c_{R1-S-R2} - k_2 \cdot c_{R1-SO-R2} - k_3 \cdot c_{R1-SO2-R2}. \end{aligned} \tag{5.10}$$

[1] Compare, formally, the transition behaviour of the Langmuir adsorption isotherm.

The solution of the equation system (5.6), (5.7) and (5.8) gives

$$c_{\mathrm{R1-S-R2}}/(c_{\mathrm{R1-S-R2}})_0 = \mathrm{EXP}(-k_1 \cdot t) \tag{5.11}$$

$$c_{\mathrm{R1-SO-R2}}/(c_{\mathrm{R1-S-R2}})_0 = k_1/(k_2 - k_1) \cdot [\mathrm{EXP}(-k_1 \cdot t) - \mathrm{EXP}(-k_2 \cdot t)] \tag{5.12}$$

$$\begin{aligned} c_{\mathrm{R1-SO2-R2}}/(c_{\mathrm{R1-S-R2}})_0 = {} & k_1 \cdot k_2 \cdot (k_2 - k_1)^{-1} \cdot \Big[(k_2 - k_3)^{-1} \cdot \mathrm{EXP}(-k_2 \cdot t) \\ & -(k_1 - k_3)^{-1} \cdot \mathrm{EXP}(-k_1 \cdot t) + (k_2 - k_1) \\ & \cdot (k_1 - k_3)^{-1} \cdot (k_2 - k_3)^{-1} \cdot \mathrm{EXP}(-k_3 \cdot t)\Big] \\ = {} & k_1 \cdot k_2 \cdot (k_2 - k_1)^{-1} \cdot (k_1 - k_3)^{-1} \cdot (k_2 - k_3)^{-1} \\ & \cdot [(k_1 - k_3) \cdot \mathrm{EXP}(-k_2 \cdot t) - (k_2 - k_3) \\ & \cdot \mathrm{EXP}(-k_1 \cdot t) + (k_2 - k_1) \cdot \mathrm{EXP}(-k_3 \cdot t)]. \end{aligned} \tag{5.13}$$

The relative concentrations $c_{\mathrm{R1'-R2'SO3H-R3'}}/(c_{\mathrm{R1-S-R2}})_0$ and $c_{\mathrm{H2O2}}/(c_{\mathrm{R1-S-R2}})_0$ result from the mol balance in the following way:

- Integration of the sum of (5.6), (5.7), (5.8) and (5.9) gives

$$\begin{aligned} 0 = {} & \left[c_{\mathrm{R1-S-R2}} - (c_{\mathrm{R1-S-R2}})_0\right] + \left[c_{\mathrm{R1-SO-R2}} - (c_{\mathrm{R1-SO-R2}})_0\right] + \\ & + \left[c_{\mathrm{R1-SO2-R2}} - (c_{\mathrm{R1-SO2-R2}})_0\right] + \Big[c_{\mathrm{R1'-R2'-SO3H-R3'}} \\ & - \left(c_{\mathrm{R1'-R2'-SO3H-R3'}}\right)_0\Big]. \end{aligned}$$

or with (5.11), (5.12), (5.13) and

$$(c_{\mathrm{R1-SO-R2}})_0 = (c_{\mathrm{R1-SO2-R2}})_0 = \left(c_{\mathrm{R1'-R2'-SO3H-R3'}}\right)_0] = 0$$

it follows that

$$\begin{aligned} c_{\mathrm{R1'-R2'-SO3H-R3'}}/(c_{\mathrm{R1-S-R2}})_0 = {} & 1 + (k_2 - k_1)^{-1} \cdot [k_1 \cdot \mathrm{EXP}(-k_2 \cdot t) - k_2 \cdot \mathrm{EXP}(-k_1 \cdot t)] \\ & + k_1 \cdot k_2 \cdot (k_2 - k_1)^{-1} \cdot \left[(k_1 - k_3)^{-1} \cdot \mathrm{EXP}(-k_1 \cdot t)\right. \\ & - (k_2 - k_3)^{-1} \cdot \mathrm{EXP}(-k_2 \cdot t) - (k_2 - k_1) \\ & \left. \cdot (k_1 - k_3)^{-1} \cdot (k_2 - k_3)^{-1} \cdot \mathrm{EXP}(-k_3 \cdot t)\right] \\ = {} & 1 + (k_2 - k_1)^{-1} \cdot [k_1 \cdot \mathrm{EXP}(-k_2 \cdot t) \\ & - k_2 \cdot \mathrm{EXP}(-k_1 \cdot t)] - k_1 \cdot k_2 \cdot (k_2 - k_1) \\ & \cdot (k_1 - k_3)^{-1} \cdot (k_2 - k_3)^{-1} \cdot [(k_1 - k_3) \\ & \cdot \mathrm{EXP}(-k_2 \cdot t) - (k_2 - k_3) \cdot \mathrm{EXP}(-k_1 \cdot t) \\ & + (k_2 - k_1) \cdot \mathrm{EXP}(-k_3 \cdot t)]. \end{aligned} \tag{5.14}$$

- By the addition of (5.9) and (5.10), subtraction of (5.7) and 2·(5.6) and integration of the result we obtain

$$\left[c_{\mathrm{H2O2}} - (c_{\mathrm{H2O2}})_0\right] + \left[c_{\mathrm{R1'-R2'-SO3H-R3'}} - \left(c_{\mathrm{R1'-R2'-SO3H-R1'}}\right)_0\right] - \left[c_{\mathrm{R1-SO-R2}} - (c_{\mathrm{R1-SO-R2}})_0\right] - 2 \cdot \left[c_{\mathrm{R1-S-R2}} - (c_{\mathrm{R1-S-R2}})_0\right] = 0$$

or with (5.11), (5.12), (5.13) and $\left(c_{\mathrm{R1'-R2'-SO3H-R3'}}\right)_0 = (c_{\mathrm{R1-SO-R2}})_0 = 0$ it follows that

$$\begin{aligned}
c_{\mathrm{H2O2}}/(c_{\mathrm{R1-S-R2}})_0 = (c_{\mathrm{H2O2}})_0/(c_{\mathrm{R1-S-R2}})_0 - 3 + \{&(k_1 - k_2)^{-1} \cdot [k_1 \cdot \mathrm{EXP}(-k_2 \cdot t) - k_2 \cdot \mathrm{EXP}(-k_1 \cdot t)] \\
&+ k_1 \cdot k_2 \cdot (k_1 - k_2)^{-1} \cdot (k_1 - k_3)^{-1} \cdot (k_2 - k_3)^{-1} \\
&\cdot [(k_2 - k_3) \cdot \mathrm{EXP}(-k_1 \cdot t) - (k_1 - k_3) \cdot \mathrm{EXP}(-k_2 \cdot t) \\
&-(k_2 - k_1) \cdot \mathrm{EXP}(-k_3 \cdot t)]\} - k_1 \cdot (k_1 - k_2)^{-1} \\
&\cdot [\mathrm{EXP}(-k_1 \cdot t) - \mathrm{EXP}(-k_2 \cdot t)] + 2 \cdot \mathrm{EXP}(-k_1 \cdot t) \\
= \left[(c_{\mathrm{H2O2}})_0/(c_{\mathrm{R1-S-R2}})_0 - 3\right] &+ \left[2 + k_1 \cdot k_2 \cdot (k_1 - k_2)^{-1} \cdot (k_1 - k_3)^{-1} - k_1 \cdot (k_1 - k_2)^{-1} - k_2 \cdot (k_1 - k_2)^{-1}\right] \\
&\cdot \mathrm{EXP}(-k_1 \cdot t) + \left[2 \cdot k_1 \cdot (k_1 - k_2)^{-1} - k_1 \cdot k_2 \cdot (k_1 - k_2)^{-1} \cdot (k_2 - k_3)^{-1}\right] \\
&\cdot \mathrm{EXP}(-k_2 \cdot t) + \left[k_1 \cdot k_2 \cdot (k_2 - k_3)^{-1} \cdot (k_1 - k_3)^{-1}\right] \cdot \mathrm{EXP}(-k_3 \cdot t) \\
= \left[(c_{\mathrm{H2O2}})_0/(c_{\mathrm{R1-S-R2}})_0 - 3\right] &+ A_1 \cdot \mathrm{EXP}(-k_1 \cdot t) + A_2 \cdot \mathrm{EXP}(-k_2 \cdot t) + A_3 \\
&\cdot \mathrm{EXP}(-k_3 \cdot t) \\
= \left[(c_{\mathrm{H2O2}})_0/(c_{\mathrm{R1-S-R2}})_0 - 3\right] &+ F_1(t) + F_2(t) + F_3(t). \qquad (5.15)
\end{aligned}$$

The value 3 corresponds to the stoichiometric coefficient of hydrogen peroxide in the overall reaction $\mathrm{R_1 - S - R_2} + 3\mathrm{H_2O_2} \rightarrow \mathrm{R_1' - R_2' - SO_3H - R_3'}$. $\left[(c_{\mathrm{H2O2}})_0/(c_{\mathrm{R1-S-R2}})_0 - 3\right]$ represents the final, relative concentration of $\mathrm{H_2O_2}$ after the complete oxidation of the batch. The concentration drops during the conversion monotonously to the final concentration according to (5.15). When the injected relative amount of the hydrogen peroxide exceeds the stoichiometric value 3, its final relative concentration is greater than zero: $\left\{(c_{\mathrm{H2O2}})_{\mathrm{E}}/(c_{\mathrm{R1-S-R2}})_0 > 0\right\}$. When the injected relative amount of the hydrogen peroxide is smaller than 3, $\left\{(c_{\mathrm{H2O2}})_0/(c_{\mathrm{R1-S-R2}})_0 < 3\right\}$, we obtain formally a negative final concentration: $\left\{(c_{\mathrm{H2O2}})_{\mathrm{E}}/(c_{\mathrm{R1-S-R2}})_0 < 0\right\}$. However, the concentration reaches a value of zero at time $t_{\mathrm{E}} < \infty$, i.e. the injected $\mathrm{H_2O_2}$ is used up and the oxidation stops abruptly at time t_{E} (in reality: in the form of a curve sharply sloping to zero in shortest time).

Hence, the procedure for determining the rate coefficients k_1, k_2, k_3 is obvious:

The plot of $\ln\left\{3 - (c_{\mathrm{H2O2}})_0/(c_{\mathrm{R1-S-R2}})_0\right\}$ versus the measured points of time t_{E} of the ends of the reaction yields, according to (5.15), a curved line which turns into a straight line F_{slowest} (Fig. 5.2) whose slope corresponds to the rate coefficient of the slowest reaction, i.e. k_1, k_2 or k_3. The point of interception with the ordinate is either

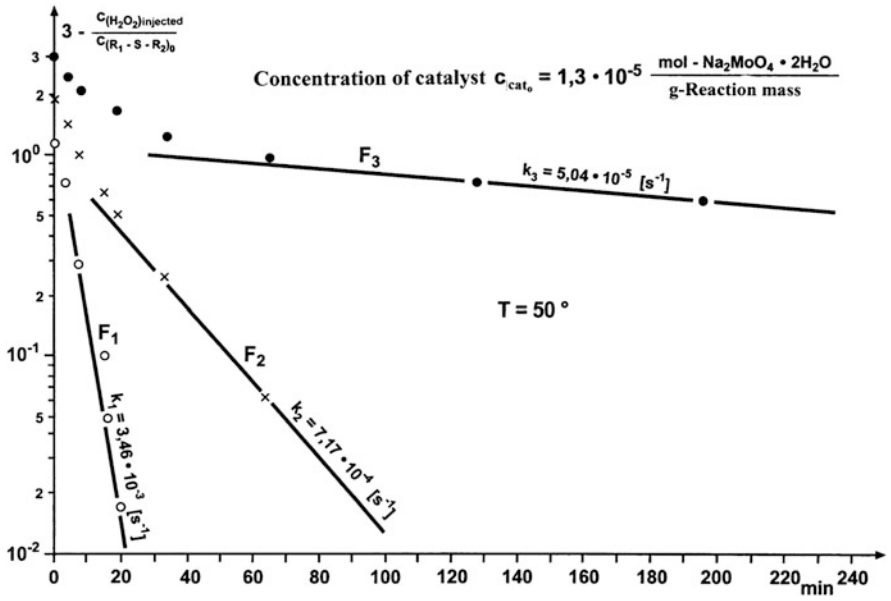

Fig. 5.2 Test of reaction model, determination of rate coefficients

$$\ln\{A_1\} = \ln\Big\{2 + k_1 \cdot k_2 \cdot (k_1 - k_2)^{-1} \cdot (k_1 - k_3)^{-1} - k_1 \cdot (k_1 - k_2)^{-1} - k_2 \cdot (k_1 - k_2)^{-1}\Big\}.$$

or

$$\ln\{A_2\} = \ln\Big\{2 \cdot k_1 \cdot (k_1 - k_2)^{-1} - k_1 \cdot k_2 \cdot (k_1 - k_2)^{-1} \cdot (k_2 - k_3)^{-1}\Big\} \quad (5.16)$$

or

$$\ln\{A_3\} = \Big\{k_1 \cdot k_2 \cdot (k_2 - k_3)^{-1} \cdot (k_1 - k_3)^{-1}\Big\},$$

depending on whether the first stage (formation of sulphoxid), the second stage (formation of sulphon) or the third stage (formation of sulpho acid) is the slowest step.

The plot of $\ln\big\{\big[3 - (c_{H2O2})_0/(c_{R1-S-R2})_0\big] - F_{slowest}\big\}$ against t_E gives a curve which also turns into a straight line $F_{second\ slowest}$ whose slope corresponds to the rate coefficient of the second slowest step. The slope can be k_1, k_2 or k_3 and the point of intersection with the ordinate can be

$$\ln\{A_1\} = \ln\Big\{2 + k_1 \cdot k_2 \cdot (k_1 - k_2)^{-1} \cdot (k_1 - k_3)^{-1} - k_1 \cdot (k_1 - k_2)^{-1} - k_2 \cdot (k_1 - k_2)^{-1}\Big\}.$$

or

$$\ln\{A_2\} = \ln\left\{2 \cdot k_1 \cdot (k_1 - k_2)^{-1} - k_1 \cdot k_2 \cdot (k_1 - k_2)^{-1} \cdot (k_2 - k_3)^{-1}\right\}$$

or

$$\ln\{A_3\} = \left\{k_1 \cdot k_2 \cdot (k_2 - k_3)^{-1} \cdot (k_1 - k_3)^{-1}\right\}.$$

Also, the plot of $\ln\left\{\left[3 - (c_{\mathrm{H2O2}})_0/(c_{\mathrm{R1-S-R2}})_0\right] - F_{\text{slowest}} - F_{\text{second slowest}}\right\}$ against t_{E} gives a straight line F_{quick}. Its slope corresponds to the rate coefficient of the quickest step, i.e. k_1 or k_2 or k_3. The point of intersection with the ordinate is either

$$\ln\{A_1\} = \ln\left\{2 + k_1 \cdot k_2 \cdot (k_1 - k_2)^{-1} \cdot (k_1 - k_3)^{-1} - k_1 \cdot (k_1 - k_2)^{-1} - k_2 \cdot (k_1 - k_2)^{-1}\right\}.$$

or

$$\ln\{A_2\} = \ln\left\{2 \cdot k_1 \cdot (k_1 - k_2)^{-1} - k_1 \cdot k_2 \cdot (k_1 - k_2)^{-1} \cdot (k_2 - k_3)^{-1}\right\}$$

or

$$\ln\{A_3\} = \left\{k_1 \cdot k_2 \cdot (k_2 - k_3)^{-1} \cdot (k_1 - k_3)^{-1}\right\}.$$

It is impossible to recognize directly the slowest, second slowest or quick reaction stage. This takes place indirectly. For that, an assumption on is made a trial basis assigning k_1, k_2 and k_3 to the slopes of the three straight lines F. By that is made simultaneously the assignment of $\ln A_1$, $\ln A_2$ and $\ln A_3$ to the corresponding points of the intersection of the straight lines with the ordinate. Then it is tested whether the calculated $\ln A_i$ and the measured intersection points coincide. If not, a second, different assignment is made, and so on. At most six different assumptions are checked.

Figures 5.2 and 5.3 show the plots of $\ln\left\{3 - (c_{\mathrm{H2O2}})_0/(c_{\mathrm{R1-S-R2}})_0\right\}$ versus t_{E} for the measured data at temperatures $T = 25$ °C and $T = 50$ °C. The result of the trial-and-error procedure gives $k_1 \gg k_2 > k_3$.

Now, on the basis of the known rate coefficients k_1, k_2 and k_3, the heats of reaction can be determined as follows. Due to (4.7), (4.34), (5.4), (5.11), (5.12) and (5.13), the determining equation of the thermal reaction power reads

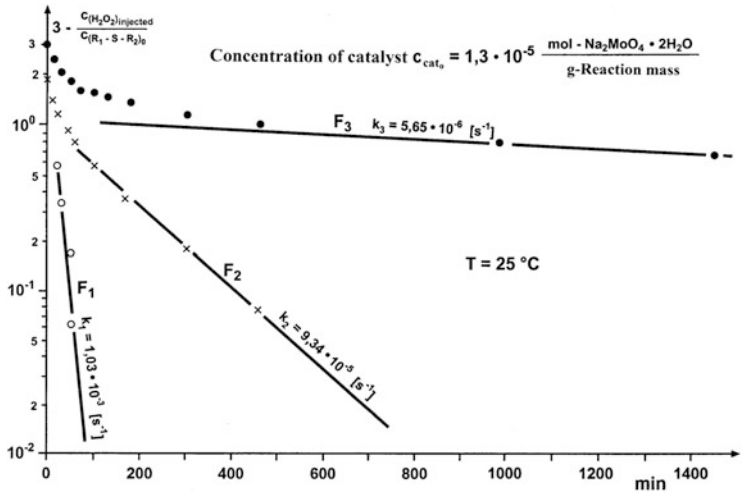

Fig. 5.3 Examination of reaction model, determination of rate coefficients k

$$
\begin{aligned}
q &= q_1 + q_2 + q_3 \\
&= r_1 \cdot (-\Delta H_{\lambda 1}) \cdot V + r_2 \cdot (-\Delta H_{\lambda 2}) \cdot V + r_3 \cdot (-\Delta H_{\lambda 3}) \cdot V \\
&= k_1 \cdot c_{\mathrm{R1-S-R2}} \cdot (-\Delta H_{\lambda 1}) \cdot V + k_2 \cdot c_{\mathrm{R1-SO-R2}} \cdot (-\Delta H_{\lambda 2}) \cdot V + k_3 \cdot c_{\mathrm{R1-SO2-R2}} \\
&\quad \cdot (-\Delta H_{\lambda 3}) \cdot V \\
&= k_1 \cdot (c_{\mathrm{R1-S-R2}})_0 \cdot V \cdot (-\Delta H_{\lambda 1}) \cdot \mathrm{EXP}(-k_1 \cdot t) \\
&\quad + k_2 \cdot k_1 \cdot (k_2 - k_1)^{-1} \cdot (c_{\mathrm{R1-S-R2}})_0 \cdot V \cdot (-\Delta H_{\lambda 2}) \cdot [\mathrm{EXP}(-k_1 \cdot t) - \mathrm{EXP}(-k_2 \cdot t)] \\
&\quad + k_1 \cdot k_2 \cdot k_3 \cdot (k_2 - k_1)^{-1} \cdot (k_1 - k_3)^{-1} \cdot (k_2 - k_3)^{-1} \cdot (c_{\mathrm{R1-S-R2}})_0 \cdot V \cdot (-\Delta H_{\lambda 3}) \\
&\quad \cdot [(k_1 - k_3) \cdot \mathrm{EXP}(-k_2 \cdot t) - (k_2 - k_3) \cdot \mathrm{EXP}(-k_1 \cdot t) + (k_2 - k_1) \cdot \mathrm{EXP}(-k_3 \cdot t)] \\
&= k_1 \cdot (-\Delta H_{\lambda 1}) + k_2 \cdot k_1 \cdot (k_2 - k_1)^{-1} \cdot (-\Delta H_{\lambda 2}) - k_1 \cdot k_2 \cdot k_3 \cdot (k_2 - k_1)^{-1} \cdot \\
&\quad (k_1 - k_3)^{-1} \cdot (-\Delta H_{\lambda 3}) \cdot (c_{\mathrm{R1-S-R2}})_0 \cdot V \cdot \mathrm{EXP}(-k_1 \cdot t) \\
&\quad + k_1 \cdot k_2 \cdot k_3 \cdot (k_2 - k_1)^{-1} \cdot (k_2 - k_3)^{-1} \cdot (-\Delta H_{\lambda 3}) - k_2 \cdot k_1 \cdot (k_2 - k_1)^{-1} \cdot \\
&\quad (-\Delta H_{\lambda 2}) \cdot (c_{\mathrm{R1-S-R2}})_0 \cdot V \cdot \mathrm{EXP}(-k_2 \cdot t) \\
&\quad + k_1 \cdot k_2 \cdot k_3 \cdot (k_1 - k_3)^{-1} \cdot (k_2 - k_3)^{-1} \cdot (-\Delta H_{\lambda 3}) \cdot (c_{\mathrm{R1-S-R2}})_0 \cdot V \cdot \mathrm{EXP}(-k_3 \cdot t) \\
&= B_1 \cdot \mathrm{EXP}(-k_1 \cdot t) + B_2 \cdot \mathrm{EXP}(-k_2 \cdot t) + B_3 \cdot \mathrm{EXP}(-k_3 \cdot t) \\
&= \boldsymbol{I}_1(t) + \boldsymbol{I}_2(t) + \boldsymbol{I}_3(t).
\end{aligned}
\tag{5.17}
$$

Plotting $\ln\{q\}$ versus time t (Fig. 5.4) yields a curved line which turns into a straight line. Its slope gives the value of the rate coefficient of the slowest stage, i.e. k_3 as determined. Hence, the straight line represents $\ln\{I_3(t)\}$ and the point of its intercept with the ordinate is, according to (5.17),

$$
\begin{aligned}
\ln\{B_3\} \;=\; & \ln\big\{(k_1 \cdot k_2 \cdot k_3 \cdot (k_1 - k_3)^{-1} \cdot (k_2 - k_3)^{-1} \cdot (-\Delta H_{\lambda 3}) \\
& \cdot (c_{\mathrm{R1-S-R2}})_0 \cdot V\big\}.
\end{aligned}
$$

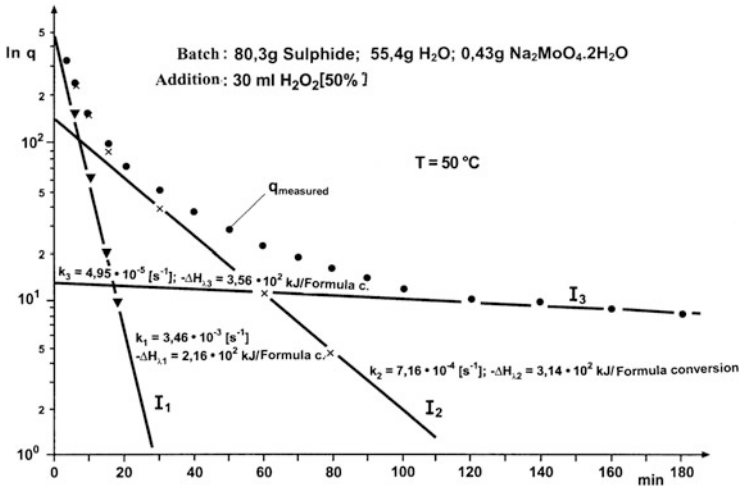

Fig. 5.4 Determination of enthalpies of reaction from course of thermal reaction power

The plot of $\ln\{(q - I_3)\}$ against time t gives a curve ending as a straight line whose slope corresponds to the rate coefficients of the second slowest reaction, i.e. k_2. Therefore, the straight line tallies with $\ln\{I_2(t)\}$ and the point of its intercept with the ordinate is in accordance with (5.17)

$$\ln\{B_2\} = \ln\Big\{\Big[k_1 \cdot k_2 \cdot k_3 \cdot (k_2 - k_1)^{-1} \cdot (k_2 - k_3)^{-1} \cdot (-\Delta H_{\lambda 3}) - k_2 \cdot k_1 \cdot (k_2 - k_1)^{-1} \cdot (-\Delta H_{\lambda 2})\Big] \cdot (c_{\mathrm{R1-S-R2}})_0 \cdot V\Big\}.$$

From the plot of $\ln\{(q - I_3 - I_2)\}$ versus t we get a straight line. Its slope corresponds with the rate coefficient of the quick stage, i.e. k_1, as determined previously. The ordinate intercept is, according to (5.17),

$$\ln\{B_1\} = \ln\Big\{\big[k_1 \cdot (-\Delta H_{\lambda 1}) + k_2 \cdot k_1 \cdot (k_2 - k_1)^{-1} \cdot (-\Delta H_{\lambda 2}) - k_1 \cdot k_2 \cdot k_3 \cdot (k_2 - k_1)^{-1} \cdot (k_1 - k_3)^{-1} \cdot (-\Delta H_{\lambda 3})\big] \cdot (c_{\mathrm{R1-S-R2}})_0 \cdot V\Big\}.$$

Using the relations B_3, B_2 and B_1 as well as the rate coefficients k_1, k_2 and k_3 we calculate the enthalpies of reaction:

$$(-\Delta H_{\lambda 1}) = 216 \ \mathrm{kJ/formula\ \ conversion},$$
$$(-\Delta H_{\lambda 2}) = 314 \ \mathrm{kJ/formula\ \ conversion},$$
$$(-\Delta H_{\lambda 3}) = 356 \ \mathrm{kJ/formula\ \ conversion}.$$

Checking whether the linear dependence of the rate coefficients on the concentration of catalyst c_{Cat_0} is valid – as the first elementary hypothesis of the catalytic

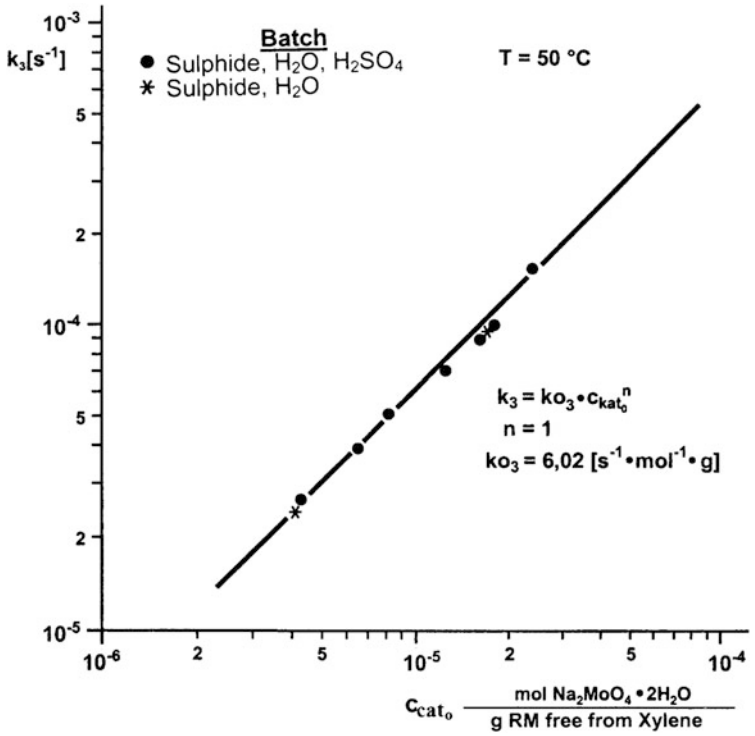

Fig. 5.5 Dependency of rate coefficient k_3 on concentration of catalyst c_{Cat_0}

elementary mechanism entails – the oxidation is carried out at different concentrations of the catalyst. Figures 5.5, 5.6, 5.7 and 5.8 show that the linear dependence applies only for the formation in sulpho acid. For the formation in sulphoxid respectively sulphon acid the dependencies of the rate coefficients on c_{Cat_0} have the powers 1.1 respectively 1.5.

Obviously, the reaction rates are overall rates which describe the dynamics of the oxidation sufficiently, see footnote[11] in 4.2.1.1.1.2.

Figures 5.5, 5.6, 5.7 and 5.8 show furthermore that the addition of either sulphuric acid or xylene does not have any effect on the value of the rate coefficients. They are only a function of the temperature and concentration of the catalyst. The Arrhenius equation (Fig. 5.9) describes the temperature dependency. Hence,

$$\begin{aligned} k_1 &= ko_1(T) \cdot c_{\mathrm{Cat}_0}^{1.1} = kH_1 \cdot \mathrm{EXP}(-E_1/RT) \cdot c_{\mathrm{Cat}_0}^{1.1}, \\ k_2 &= ko_2(T) \cdot c_{\mathrm{Cat}_0}^{1.5} = kH_2 \cdot \mathrm{EXP}(-E_2/RT) \cdot c_{\mathrm{Cat}_0}^{1.5}, \\ k_3 &= ko_3(T) \cdot c_{\mathrm{Cat}_0} = kH_3 \cdot \mathrm{EXP}(-E_3/RT) \cdot c_{\mathrm{Cat}_0}, \end{aligned} \tag{5.18}$$

with

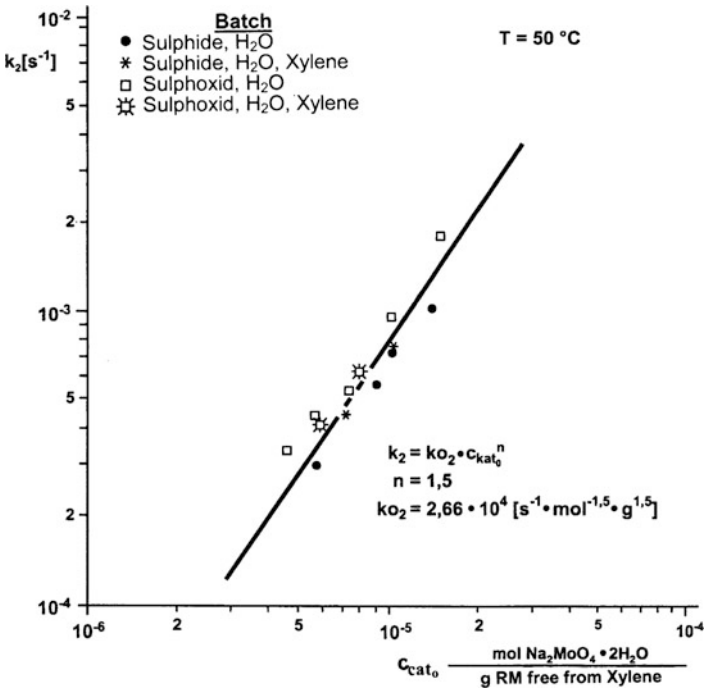

Fig. 5.6 Dependency of rate coefficient k_2 on concentration of catalyst c_{Cat_0}

$$kH_1 = 2.05 \times 10^9 \left[\mathrm{s}^{-1}\ \mathrm{mol}^{-1.1}\ \mathrm{g}^{1.1}\right], E_1 = 38.78\ \mathrm{kJ/mol},$$
$$kH_2 = 5.45 \times 10^{14} \left[\mathrm{s}^{-1}\mathrm{mol}^{-1.5}\ \mathrm{g}^{1.5}\right], E_2 = 63.76\ \mathrm{kJ/mol},$$
$$kH_3 = 1.29 \times 10^{12} \left[\mathrm{s}^{-1}\mathrm{mol}^{-1}\ \mathrm{g}^{1}\right], E_3 = 70.04\ \mathrm{kJ/mol}.$$

The different values of the activity energy E_1, E_2 and E_3 causes the rate of formation in the desired product sulphon to increase by increasing the temperature at a rate which is greater than the rate of sulphon formation, so that the greatest possible yield of sulfphon is reduced by increasing the temperature. Admittedly, the maximum yield is not only affected by the temperature but also by the amount of added catalyst, because of the different dependencies of the rates of formation and consumption on the concentration of the catalyst. By increasing the concentration of the catalyst, the rate of formation in sulphon increases more than the rate of its consumption. For a given temperature and used amount of catalyst the maximum yield is reached at an optimal time t_{opt}.

For a discontinuous conversion the optimal reaction time t_{opt} batch is found by differentiating (5.13) and setting to zero

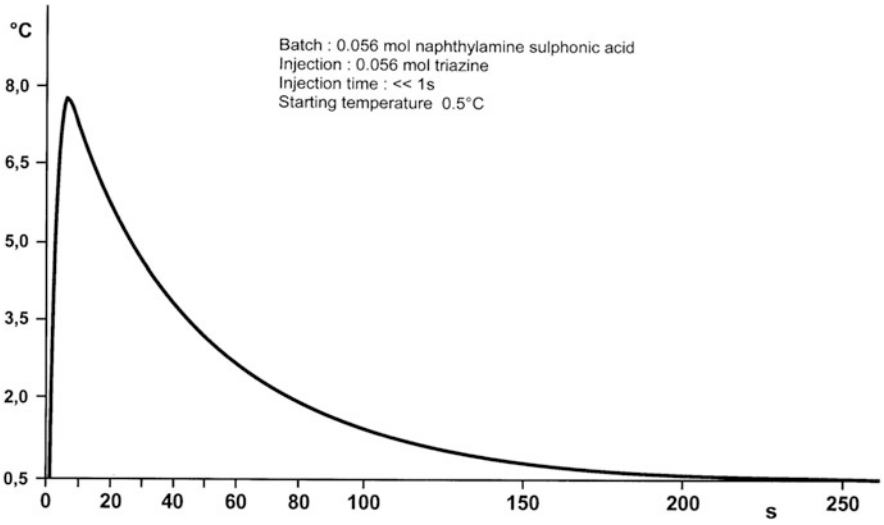

Fig. 5.7 Dependency of rate coefficient k_1 on concentration of catalyst c_{Cat_0}

$$k_1 \cdot (k_2 - k_3) \cdot \mathrm{EXP}\left[(k_3 - k_1) \cdot t_{\mathrm{opt}}\right] - k_2 \cdot (k_1 - k_3) \cdot \mathrm{EXP}\left[(k_3 - k_2) \cdot t_{\mathrm{opt}}\right] = k_3 \cdot (k_2 - k_1). \tag{5.19}$$

Rearrangement of the relation to the explicit expression $t_{\mathrm{opt}} = f_2(k_1, k_2, k_3)$ is not possible. Nevertheless, because of the elaborated kinetic fact that $k_1 \gg k_2,\ k_3$, a direct calculation with sufficient accuracy is possible; $k_1 \gg k_2,\ k_3$ means that the formation of sulphoxid from sulphide occurs – compared with the following relatively slow reactions to sulphon and sulpho acid – almost instantly (Fig. 5.10). Because of that, the exact equation (5.19) shrinks in good approximation to

$$-k_2 \cdot k_1 \cdot \mathrm{EXP}\left[(k_3 - k_2) \cdot t_{\mathrm{opt}}\mathrm{batch} \cong -k_3 \cdot k_1.\right.$$

Corresponding to the slowness of the consecutive stages, no distinct peak exists; rather, there is an elongated maximum. Hence, its temporal position is sufficiently precisely determined by

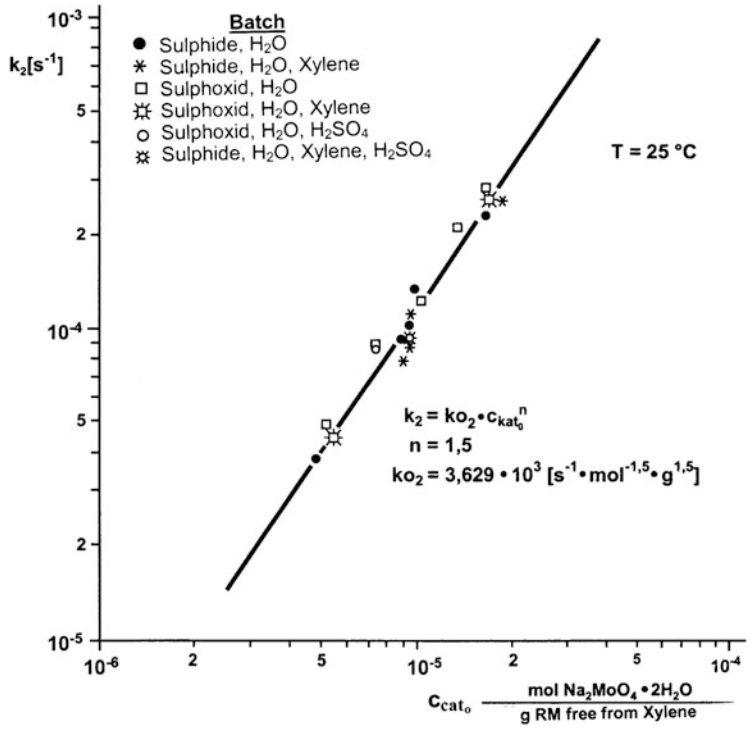

Fig. 5.8 Dependency of rate coefficient k_2 on concentration of catalyst $c_{\mathrm{Cat_0}}$

$$t_{\mathrm{opt}}\mathrm{batch} = \ln(k_3/k_2)/(k_3 - k_2). \tag{5.20}$$

The combination of (5.18) and (5.20) gives t_{opt} batch as a function of the temperature and concentration of the catalyst:

$$t_{\mathrm{opt}}\mathrm{batch} = kH_3/kH_2 \cdot \mathrm{EXP}[(E_2 - E_3)/RT] \cdot c_{\mathrm{Cat_0}}^{-0.5} \Big/ \left(kH_3 \cdot \mathrm{EXP}[-E_3/RT] \cdot c_{\mathrm{Cat_0}} - kH_2 \cdot \mathrm{EXP}[-E_2/RT] \cdot c_{\mathrm{Cat_0}}^{1.5}\right). \tag{5.21}$$

Combining (5.13), (5.20) and (5.21) and considering $k_1 \gg k_2$, k_3 yields the maximum concentration of the desired product sulphon as a function of temperature and amount of catalyst:

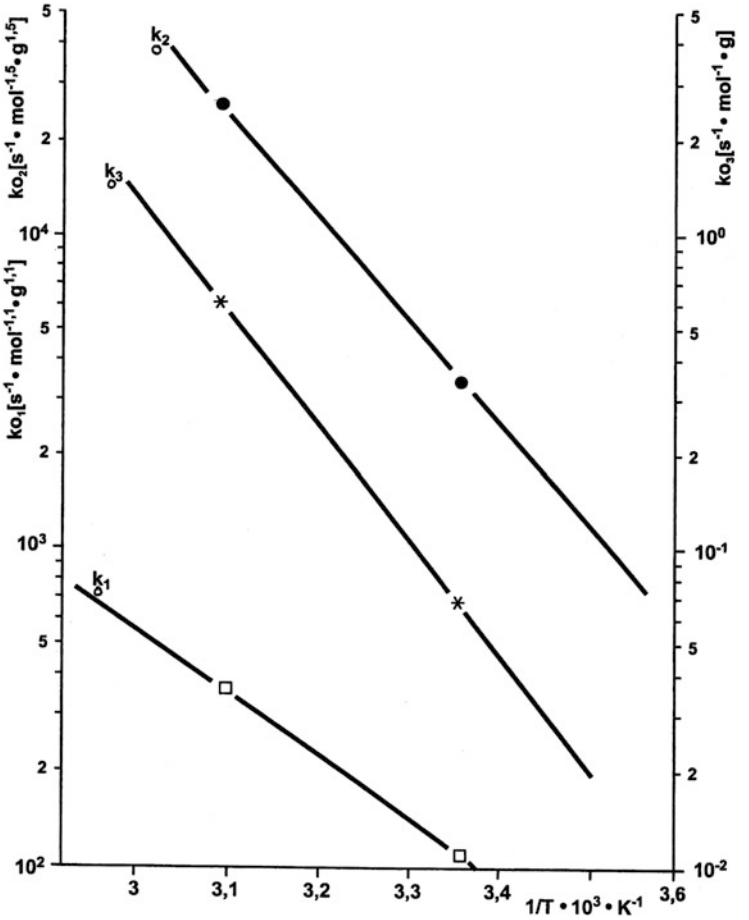

Fig. 5.9 Dependency on temperature of rate coefficients ko_1, ko_2 and ko_3 according to Arrhenius relation

$$\begin{aligned}
\left[c_{\mathrm{R1-SO2-R2}}/(c_{\mathrm{R1-S-R2}})_0\right]_{\max} &= S_{\max} \\
&= k_2/(k_3-k_2)\cdot\left\{\mathrm{EXP}\left[k_2\cdot t_{\mathrm{opt}}\mathrm{batch}\right]-\mathrm{EXP}\left[k_3\cdot t_{\mathrm{opt}}\mathrm{batch}\right]\right\} \\
&= k_2/(k_3-k_2)\cdot\left[(k_3/k_2)^{-k_2/(k_3-k_2)}-(k_3/k_2)^{-k_3/(k_3-k_2)}\right] \\
&= (k_2/k_3)^{k_3/(k_3-k_2)} \\
= \left\{kH_2/kH_3\cdot\mathrm{EXP}[(E_3-E_2)/RT]\cdot {c_{\mathrm{Cat}_0}}^{0.5}\right\}^{1/\left(1-kH_2/kH_3\cdot\mathrm{EXP}[(E_3-E_2)/RT]\cdot {c_{\mathrm{Cat}_0}}^{0.5}\right)}&.
\end{aligned} \tag{5.22}$$

It is advisable to determine the dosage of H_2O_2 according to the amount which is consumed at the optimal oxidation time t_{opt} batch. This amount $(H_2O_2)_{\mathrm{oOptimum}}$ can

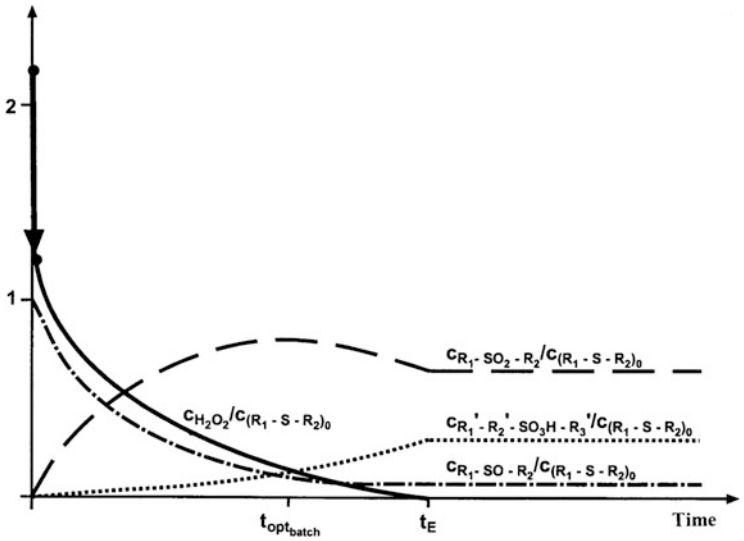

Fig. 5.10 Fundamental course of relative concentrations versus time after instantaneous dosage of H_2O_2 in a batch of R1–S–R2, by which $(c_{H2O2})_0/(c_{R1-S-R2})_0 < 3$, an isothermal, discontinuous conversion, constant-volume reaction

be calculated by setting (5.15) to zero, resolving to $(c_{H2O2})_0/(c_{R1-S-R2})_0$ using (5.22) and considering $k_1 \gg k_2, k_3$. The result is

$(c_{H2O2})_{0Optimum}/(c_{R1-S-R2})_0 = 3 - 2 \cdot \mathrm{EXP}\left[-k_2 \cdot t_{opt}\mathrm{batch}\right] - k_2/(k_2 - k_3) \cdot \left\{\mathrm{EXP}\left[-k_3 \cdot t_{opt}\mathrm{batch}\right] - \mathrm{EXP}\left[-k_2 \cdot t_{opt}\mathrm{batch}\right]\right\} = 3 - 2 \cdot \mathrm{EXP}\left[-k_2 \cdot t_{opt}\mathrm{batch}\right] - S_{max}$. The dosage of H_2O_2 at the constant rate v instead of injection increases the optimal reaction time t_{opt}. At the beginning of the total dosing time t_{Dos} the inflowing H_2O_2 oxidizes during the time $\delta t_{d0s} = V \cdot (c_{R1-S-R2})_0/(v \cdot \rho_{H2O2}/M_{H2O2})$ virtually only the batch of sulphide to sulphoxid because of $k_1 \gg k_2, k_3$. Practically, only at that point in time do consecutive oxidations start (Fig. 5.11). The following expression is valid:

$$t_{opt}\mathrm{batch} \ll t_{opt}\mathrm{semibatch} < \left(t_{opt}\mathrm{batch} + t_{dos}\right).$$

The rule of thumb gives a well-founded

$$t_{opt}\mathrm{semibatch} \cong \left(t_{opt}\mathrm{batch} + \delta t_{dos}\right).$$

Figure 5.12 shows for a batch process the temporal courses of

- The maximum concentration of sulphon R_1–SO_2–R_2
- The relevant amount of residual sulphide R_1–S–R_2
- The optimal reaction time
- The optimal amount of H_2O_2

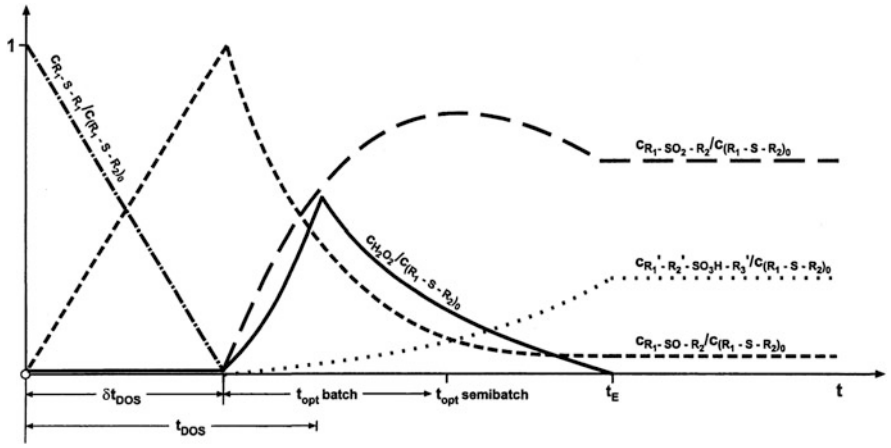

Fig. 5.11 Fundamental course of relative concentrations versus time for constant, continuous dosing of H_2O_2 in a batch of R1–S–R2, by which $(c_{H2O2})_0/(c_{R1-S-R2})_0 < 3$, in time interval t_{Dos}

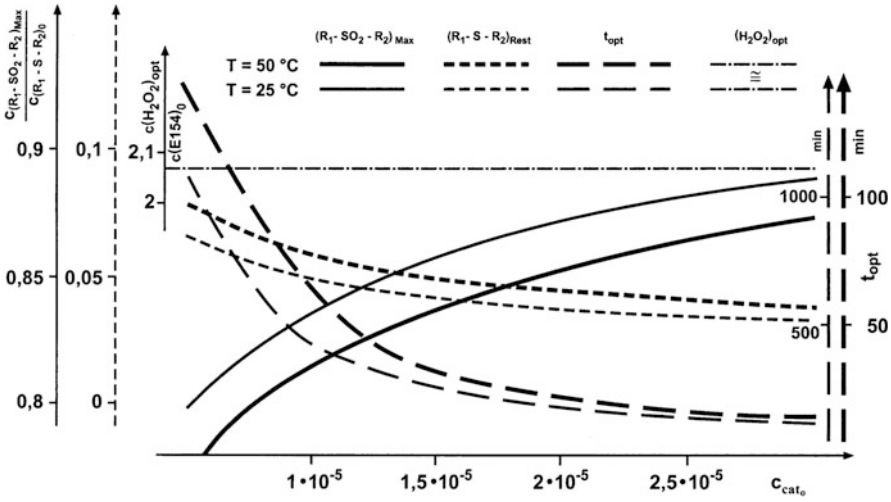

Fig. 5.12 Isothermal batch process, 25 and 50 °C, maximum concentration of sulphon $c_{R1–SO2–R2}/(c_{R1–S–R2})_0$, associated optimal reaction time t_{opt}, residual concentration of sulphide $c_{R1–S–R2}/(c_{R1–S–R2})_0$ and optimal dosage $(c_{H2O2})_0/(c_{R1–S–R2})_0$ depending on concentration of catalyst c_{Cat_0}

depending on the amount of catalyst used at temperatures of 25 and 50 °C.

Figures 5.13 and 5.14 present for both temperatures the analytically found concentrations of sulphon after consumption of H_2O_2 depending on the dosed amount of H_2O_2. Because of the scattered analyses, the optimal dosage of H_2O_2 cannot be determined exactly. Nevertheless, despite the scattered values it can be seen that the experimental results slightly exceed the optimum value calculated according to (5.13) and indicated in Fig. 5.12. The difference increases even with

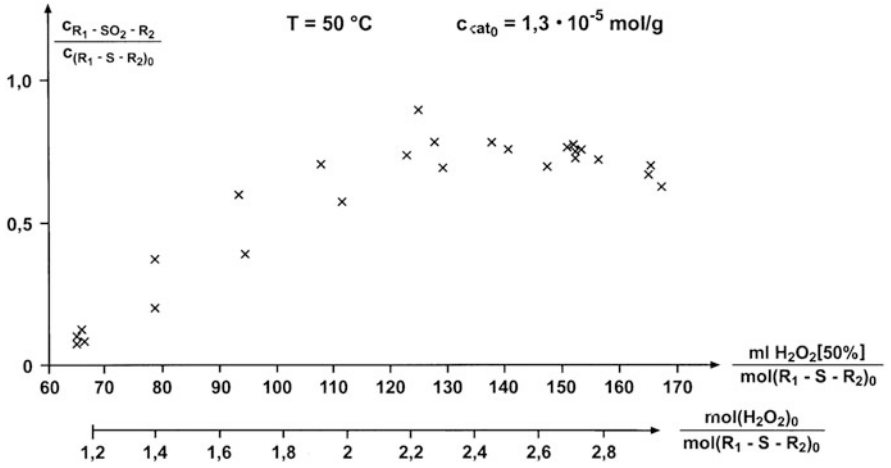

Fig. 5.13 Measured concentration $R_1 - S - R_2/(R_1 - S - R_2)_o$ depending on added amount of $H_2O_2[50\ \%], T = 50°$

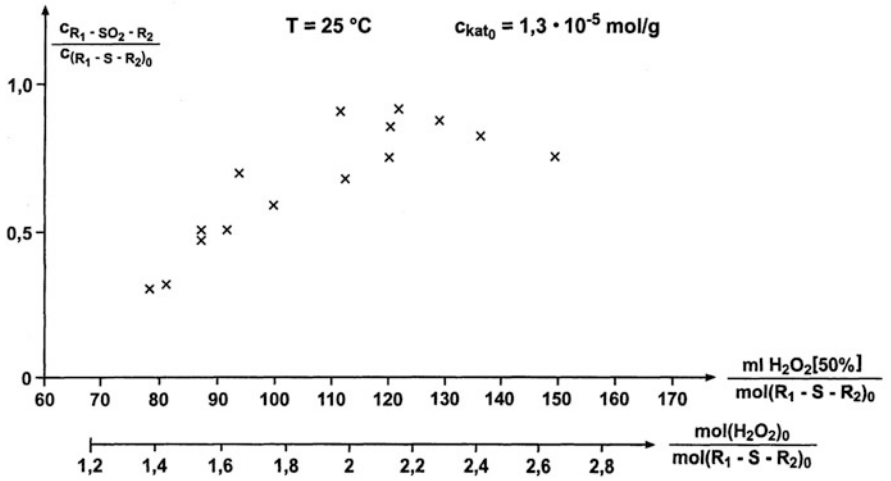

Fig. 5.14 Measured concentration $R_1 - S - R_2/(R_1 - S - R_2)_0$ depending on added amount of $H_2O_2[50\ \%], T = 25°$

the temperature. There is very good reason to suppose that the increased use of H_2O_2 is caused by the decomposition of H_2O_2, by which oxygen is released. Impurities in substances in the reaction mass (sulphide, xylene) and on the surface of the measuring-kettle wall give rise to the catalysis of the initially very small intrinsic decomposition of H_2O_2. The mingling of H_2O_2 in the filling leads to a slight increase in the pressure in the measuring kettle. Based on the rate of pressure increase, a mean formation of approximately 5×10^{-6} resp. 1×10^{-6} moles H_2O_2/s at 50 °C rsp. 25 °C is found.

5.1.2 Belousow–Zhabotinski Reaction in a Closed Reactor

One of the most interesting results of the thermodynamics of irreversible processes (thermodynamics far from equilibrium) is the realization that reaction systems in open or closed reactors under special premises are able to oscillate.[2] One of the early discovered, popular and intensively investigated reactions is the Belousow–Zhabotinski reaction. The overall process is the oxidation of malonic acid by means of bromate in sulphuric aqueous solution in the presence of the catalyst cerium:

$$2BrO_3^- + 3CH_2(COOH)_2 + 2H^+ \xrightarrow{Ce/H_2O/H_2SO_4} 2BrCH(COOH)_2 + 3CO_2 + 4H_2O.$$

During the discontinuous conversion in a closed reactor under conditions of oscillation, the reactants and the products do not perform damped oscillations, but the catalyst alternates in the time after an inducing and a finishing phase of the overall reaction rhythmically between two degrees of oxidation via certain intermediate reactions. Detailed detective work revealed that all in all 20 intermediate reactions run [12].

The course of conversion has already been photometrically, polarographically and barometrically recorded. The polarographic measurement, almost free of inertia, has revealed a sawtooth-shaped oscillation. Calorimetric investigation has been carried out until now only in micro calorimeters by differential thermal analysis DTA (non-isothermal) and by differential-scanning-calorimetry DSC (quasi-isothermal). The calorimetric inertia of the control systems is too large to enable the system to record correctly sawtooth-shaped oscillations, i.e. relatively abrupt changes in reaction power. The characteristic course can only be distortedly recorded.

The author has therefore tried to measure the thermal reaction power as well as the change in pressure due to CO_2 produced in the bench scale calorimeter TKR under virtually isothermal conditions. The level of the pH-value, prerequisite for the start of oscillations, is produced by an injection of strong concentrated sulphuric acid into the batch, which is already brought to the set temperature of the reaction. The unavoidable stroke of heat due to the abruptly released large amount of heat of dilution cannot be compensated completely, even despite having pre-chilled sulphuric acid and electric heating power p_2 temporarily reduced to zero (Fig. 5.15). The result is a large jump in temperature within the reaction mixture, so that the set temperature respectively the equilibrium of control is achieved relatively late.

During this time the induction phase of the oscillation has already finished, i.e. the oscillation is already started.

During the further, isothermal progress of the reaction the amplitude of the oscillations (recognizable by periodical cut-ins along the course of the measured thermal reaction power) increases from approximately 5 W up to approximately

[2] See Sect. 4.2.1.1.2.6.

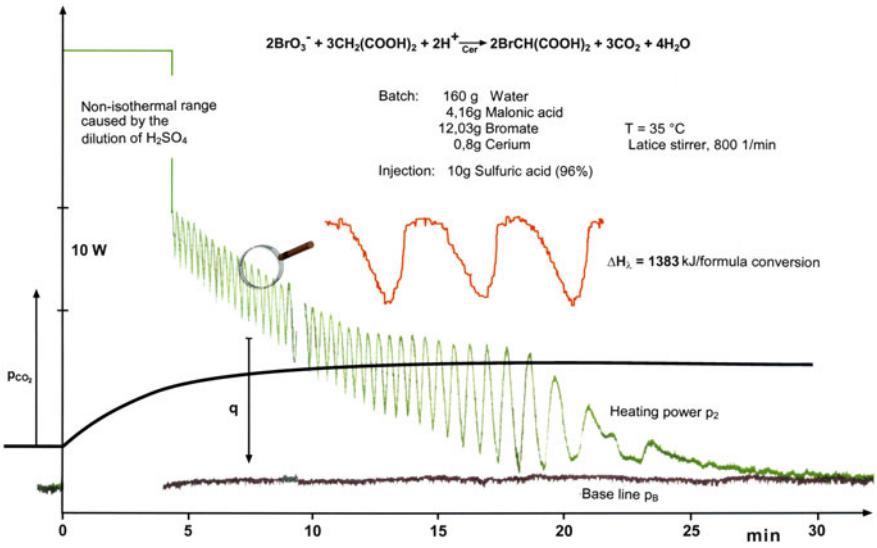

Fig. 5.15 Temporal course of thermal reaction power of Belousow–Zhabotinski reaction in a closed reactor under virtually isothermal conditions

about 10 W and then towards the end of the conversion decreases to zero. The time of oscillation increases instantly – also in the beginning phase of the descending amplitude. The slow motion reveals that the characteristic oscillation shape is similar to the usual sawtooth. From the area between the baseline p_B and the curve of the heating power p_2, both extrapolated rearwards towards the time zero, yields by approximation an overall heat of reaction of

$$-\Delta H_\lambda \cong 1,383 \ \text{kJ/formula conversion}.$$

The overall heat of reaction per mol oxidized malonic acid is

$$\begin{aligned} -\Delta H_{\text{malonic acid}} &= (-\Delta H_\lambda)/|\nu_{\text{malonic acid}}| = (-\Delta H_\lambda)/|-3| \\ &\cong 461 \ \text{kJ/mol}_{\text{malonic acid}}. \end{aligned}$$

5.1.3 *Reaction of Formic Acid with Hexamethylene-Diisocynate*

As an example of the elaboration of a reaction kinetic

- from the data of an isothermal, discontinuous conversion
- on the basis of numerical calculation

is discussed the initial phase of the multiple-stage, consecutive reaction of the aliphatic diisocynate hexamethylene-diisocyanate H and formic acid A to a variety of products P_ξ:

$$H + A \xrightarrow{NCO} P_1 \xrightarrow{NCO/P_\xi} P_2 \xrightarrow{NCO/P_\xi} P_\xi \rightarrow \ldots$$

For the thermokinetic measurement, the batch of hexamethylene-diisocyanate is brought to the reaction temperature 90 °C and a small amount of formic acid (p.a.) instantly injected to start the reaction. The injection causes an instantaneous, large heat stroke, and the pressure rises slightly. Then follows a monotonous decrease in the thermal reaction power accompanied by a slow increase in pressure. The same goes for the instant addition of larger amounts or for the successive addition of small amounts. Continuous, constant dosing causes a quick and linear temperature increase and a slow increase in the pressure. At the end of dosing the increase in temperature stops abruptly and at this moment the temperature starts to decay.

The analysis of the produced gas shows for all cases a mixture of CO_2 and CO. The relation of the components in samples of gas, taken during the further course of the reaction, changes favourably for CO.

From the heat stroke in the initial phase the quantity 59 kJ/mol_A results as heat from the process. The value is much larger than the value of a usual physicochemical process (e.g. heat of mixture).

With the purpose of reducing the dynamics of the obviously initial chemical processes, which at high temperatures evidently run almost instantly, and to have a dampening effect on the subsequent consecutive reactions the temperature is reduced to 0 °C and lower. Figure 5.16, for instance, shows the positive results. It can be seen that the thermal reaction power at first decreases monotonously, then increases, passing a peak, and then decreases again, approaching almost zero. The initial change in pressure after the injection of A is negligibly small. However, during the phase of increase in the thermal reaction power the pressure now increases quickly to achieve, after an S-shaped course, a nearly constant (i.e. minimally changing) run. In the analysis of the formed gas, a mixture of CO_2 and CO with far more than 90 % CO_2 is detected. Thus, it is assumed that during the initial phase and in particular during the following relatively short-term increase in the renewed heat release no or only an unimportant part of the injected formic acid decomposes.

A numeric method then gives a satisfying validation of the experimental results only when the following reaction mechanism is assumed. Hexamethylene-diisocyanate H and formic acid A first form the additive compound H¤A, which arranges by a further reversible step a ring R, stabilized by a hydrogen-bridge linkage.[3] The additive compound H¤A is unstable and forms, separating CO_2, the first product P_1 and in consecutive reactions a variety of products P_ξ, in Fig. 5.16 summarily denoted by

[3] In principle, the existence of the hydrogen-bridge linkage can be proved by infrared spectroscopy. At the time of the calorimetric investigation there existed only the method of IR illumination of cells. However, the IR beam was absorbed totally despite the fact that extremely thin fluid layers were used. Today the proof can easily be carried out by the attenuated total reflection infrared spectroscopy, ATR-IR method, quod sit perficiendum.

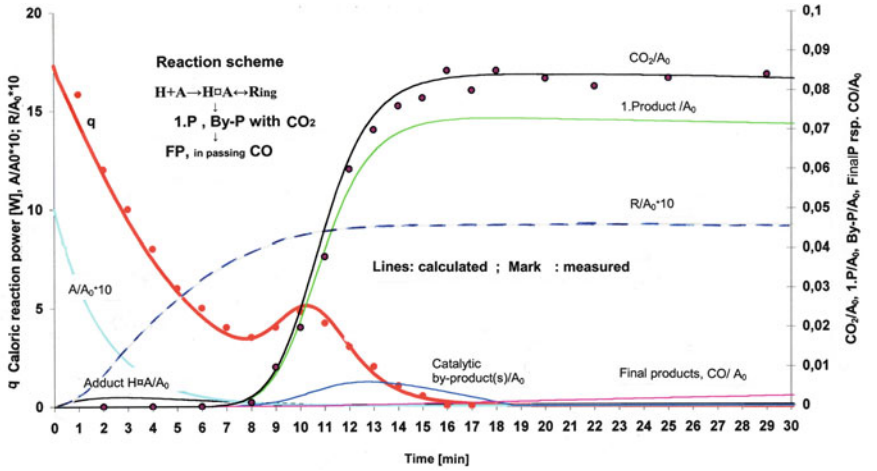

Fig. 5.16 Thermal reaction power q and relation CO_2/A_0 during reaction of hexamethylene-diisocyanate (H) and formic acid (A) p.a. 5.81 g F; 171 g H, i.e. in large excess; $T = 0$ °C; rpm = 1,500 – $\Delta H_{\lambda\text{reaction step}(n)} = 18/21/92/92$ kJ/formula conversion isothermal, discontinuous conversion. H ¤ A means additive compound of H and A

FP. However, this variety arises perceptibly only at reaction temperatures above 50 °C by consecutive reactions with the surplus hexamethylene-diisocynate. There also occur side reactions of subsequent products, separating CO.

The formation of the first product P_1 obviously occurs by autocatalysis, an usual occurrence in the chemistry of isocyanides (i.e. formation of urethane). For this formation, a relatively short-lived by-product BP is assumed with catalysing properties:

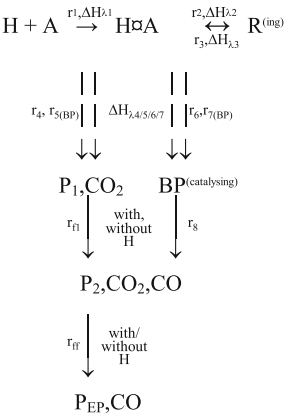

The stoichiometric coefficients are

$$
\begin{aligned}
{}_{\nu}\mathrm{A1} &= -1\,, \nu_{\mathrm{A2}} = 0, \nu_{\mathrm{A3}} = 0, \nu_{\mathrm{A4}} = 0, \nu_{\mathrm{A5}} = 0, \nu_{\mathrm{A6}} = 0, \nu_{\mathrm{A7}} = 0, \nu_{\mathrm{A8}} = 0,\\
\nu_{\mathrm{Af1}} &= 0\,, \ldots, \nu_{\mathrm{Aff}} = ?(0 \text{ at } T = 0)\\
\nu_{\mathrm{H\,\square\,A}} &= 1\,, \nu_{\mathrm{H\,\square\,A2}} = -1, \nu_{\mathrm{H\,\square\,A3}} = 1, \nu_{\mathrm{H\,\square\,A4}} = -1, \nu_{\mathrm{H\,\square\,A5}} = -1,\\
\nu_{\mathrm{H\,\square\,A6}} &= 1, \nu_{\mathrm{H\,\square\,A7}} = -1, \nu_{\mathrm{H\,\square\,A8}} = -1, \nu_{\mathrm{H\,\square\,Af1}} = 0, \ldots, \nu_{\mathrm{Aff}} = ?(0 \text{ at } T = 0)\\
\nu_{\mathrm{R1}} &= 0, \nu_{\mathrm{R2}} = 1, \nu_{\mathrm{R3}} = -1, \nu_{\mathrm{R4}} = 0, \nu_{\mathrm{R5}} = 0, \nu_{\mathrm{R6}} = 0, \nu_{\mathrm{R7}} = 0, \nu_{\mathrm{R8}} = 0,\\
\nu_{\mathrm{Rf1}} &= 0, \ldots, \nu_{\mathrm{Rff}} = ?(0 \text{ at } T = 0)\\
\nu_{\mathrm{P11}} &= 0, \nu_{\mathrm{P12}} = 0, \nu_{\mathrm{P13}} = 0, \nu_{\mathrm{P14}} = 1, \nu_{\mathrm{P15}} = 1, \nu_{\mathrm{P16}} = 0, \nu_{\mathrm{P17}} = 0,\\
\nu_{\mathrm{P18}} &= 0, \nu_{\mathrm{P1f1}} = -1, \ldots, \nu_{\mathrm{B1ff}} = ?(0 \text{ at } T = 0)\\
\nu_{\mathrm{BP1}} &= 0, \nu_{\mathrm{BP2}} = 0, \nu_{\mathrm{BP3}} = 0, \nu_{\mathrm{BP4}} = 0, \nu_{\mathrm{BP5}} = 0, \nu_{\mathrm{BP6}} = 1, \nu_{\mathrm{BP7}} = 1,\\
\nu_{\mathrm{BP8}} &= -1, \nu_{\mathrm{BPf1}} = 0\,, \ldots, \nu_{\mathrm{BPff}} = ?(0 \text{ at } T = 0)\\
\nu_{\mathrm{H1}} &= -1, \nu_{\mathrm{H2}} = 0, \nu_{\mathrm{H3}} = 0, \nu_{\mathrm{H4}} = 0, \nu_{\mathrm{H5}} = 0, \nu_{\mathrm{H6}} = 0, \nu_{\mathrm{H7}} = 0, \nu_{\mathrm{H8}} = 0,\\
\nu_{\mathrm{Hf1}} &= 0, \ldots, \nu_{\mathrm{Hff}} = ?(0 \text{ at } T = 0).
\end{aligned}
$$

According to (4.34), the rates of change in concentration are

$$
\begin{aligned}
\mathrm{d}c_{\mathrm{F}}/\mathrm{d}t &= -\,r_1,\\
\mathrm{d}c_{\mathrm{H\square F}}/\mathrm{d}t &= r_1 - r_2 + r_3 - r_4 - r_5 - r_6 - r_7,\\
\mathrm{d}c_{\mathrm{R}}/\mathrm{d}t &= r_2 - r_3,\\
\mathrm{d}c_{\mathrm{P1}}/\mathrm{d}t &= r_4 + r_5 - r_{\mathrm{f1}} (\cong 0 \text{ at } 0\ ^{\circ}\mathrm{C}),\\
\mathrm{d}c_{\mathrm{BP}}/\mathrm{d}t &= r_6 + r_7 - r_8,\\
\mathrm{d}c_{\mathrm{H}}/\mathrm{d}t &= -\,r_1 - \{r_{\mathrm{f1}} + \textstyle\sum r_{\mathrm{ff}}\} (\cong 0 \text{ at } 0\ ^{\circ}\mathrm{C}),\\
\mathrm{d}c_{\mathrm{EP}}/\mathrm{d}t &= r_8 + \{r_{\mathrm{f1}} + \textstyle\sum r_{\mathrm{ff}}\} (\cong 0 \text{ at } 0^{\circ}\mathrm{C}).
\end{aligned}
$$

Only the following expressions of the rate functions fit sufficiently the experimental results:

$$
\begin{aligned}
r_1 &= k_1^{'} \cdot c_{\mathrm{H}} (\cong \text{const at } T = 0) \cdot c_{\mathrm{A}},\ r_2 = k_2 \cdot c_{\mathrm{H\,\square\,A}},\ r_3 = k_3 \cdot c_{\mathrm{R}},\ r_4 = k_4 \cdot c_{\mathrm{H\,\square\,A}},\\
r_5 &= k_5^{'} \cdot c_{\mathrm{H\,\square\,A}} \cdot c_{\mathrm{NP}},\ r_6 = k_6 \cdot c_{\mathrm{H\,\square\,A}},\ r_7 = k_7^{'} \cdot c_{\mathrm{H\,\square\,A}} \cdot c_{\mathrm{BP}},\ r_8 = k_8 \cdot c_{\mathrm{BP}}, r_8\\
&= k_8 \cdot c_{\mathrm{BP}},\ r_{\mathrm{f1}}, r_{\mathrm{ff}} = ?(\cong 0 \text{ at } 0\ ^{\circ}C),
\end{aligned}
$$

with

$$
\begin{aligned}
k_5^{'} &= k_5/(c_{\mathrm{A}} + c_{\mathrm{H\,\square\,A}} + c_{\mathrm{R}} + c_{\mathrm{P1}} + c_{\mathrm{BP}} + c_{\mathrm{EP}}) \quad \text{respectively}\\
k_7^{'} &= k_7/(c_{\mathrm{A}} + c_{\mathrm{H\,\square\,A}} + c_{\mathrm{R}} + c_{\mathrm{P1}} + c_{\mathrm{BP}} + c_{\mathrm{EP}}).
\end{aligned}
$$

Figure 5.16 shows optimally fitted curves of a measurement at 0 °C using $k_1{}' \cdot c_{\mathrm{H0}} = k_1$, $r_{\mathrm{f1}} = k_{\mathrm{f1}} \cdot c_{\mathrm{P1}}$, $r_{\mathrm{ff}} = 0$ and the following rate coefficients and heats of reaction:

$$
\begin{aligned}
k_1 &= 8.33 \times 10^{-3}\ \mathrm{s}^{-1} & -\Delta H_{\lambda_1} &= 16.4\ \mathrm{kJ/formula\ conversion},\\
k_2 &= 4.63 \times 10^{-3}\ \mathrm{s}^{-1} & -\Delta H_{\lambda_2} &= 20.9\ \mathrm{kJ/formula\ conversion},\\
k_3 &= 4.63 \times 10^{-6}\ \mathrm{s}^{-1} & -\Delta H_{\lambda_3} &= -20.9\ \mathrm{kJ/formula\ conversion},\\
k_4 &= 1.68 \times 10^{-11}\ \mathrm{s}^{-1} & -\Delta H_{\lambda_4} &= 92.1\ \mathrm{kJ/formula\ conversion},\\
k_5 &= 1.01\ \mathrm{s}^{-1} & -\Delta H_{\lambda_5} &= 92.1\ \mathrm{kJ/formula\ conversion},\\
k_6 &= 1.28 \times 10^{-13}\ \mathrm{s}^{-1} & -\Delta H_{\lambda_6} &= 92.1\ \mathrm{kJ/formula\ conversion},\\
k_7 &= 1.39 \times 10^{-1}\ \mathrm{s}^{-1} & -\Delta H_{\lambda_7} &= 92.1\ \mathrm{kJ/formula\ conversion},\\
k_8 &= 3E-4\ \mathrm{s}^{-1} & -\Delta H_{\lambda_8} &= -,\\
k_{\mathrm{f1}} &\cong 1E-6\ \mathrm{s}^{-1} & -\Delta H_{\lambda_{\mathrm{f1}}} &= -.
\end{aligned}
$$

An ascending temperature increases the rates of the reactions as well as the catalysis. The activation temperature E/R of the intrinsic initial steps is approximately 10,000 K.

The catalysis is sensitive to foreign substances and impurities. For instance, the increase of the tiny residual concentration of oxalic acid in the usually available formic acid (p.a.) by the addition of a small amount of this acid stops the catalysis; in contrast, the addition of acetic acid, which is also present in the remained impurity of the formic acid (p.a.), does not show any effect. The catalytic process changes when the fluid residue of the distillation of formic acid (p.a.) instead of formic acid (p.a.) is used. In that case, the course of the caloric reaction power shows two, three or more consecutive wave lines and simultaneously in the course of the pressure CO_2/CO three or more successive stair lines depending on the duration of the distillation of the usually available formic acid (p.a.).

If one uses monoisocyanate (e.g. phenyl-isocyanate) instead of the aliphatic diisocyanate, catalysis does not take place, just as with toluidine-diisocyanate. In contrast, the use of isophorone-diisocyanate shows catalysis.

5.2 Non-isothermal, Discontinuous, Constant-Volume Reaction

5.2.1 Reaction of an Amine Hydrochloride and an Alkali Nitrite

As an example of a kinetic analysis of a quick reaction

- From the data of a non-isothermal, discontinuous conversion
- On the basis of mathematical-analytical relations

the irreversible conversion of an amino hydrochloride **A** and an alkali nitrite **B** in hydrochloric, aqueous solution to a heterocyclic resultant **F** is discussed.

By a first step the salt **C** is formed (as well as the by-products D and E)

$$\mathrm{A} + \mathrm{B} \xrightarrow[\mathrm{H_2O,\,HCl}]{r_1,\,\Delta \mathrm{H}_{\lambda 1}} \mathrm{C} + \mathrm{D} + \mathrm{E},$$

with

$$\text{stoichiometric coefficients} \quad v_{\mathrm{A1}} = -1, v_{\mathrm{B1}} = -1, v_{\mathrm{C1}} = 1, v_{\mathrm{D1}} = 2, v_{\mathrm{E1}} = 1.$$

In a second step the intramolecular closure of the intermediate product **C** to the desired heterocyclic, final product **F** (as well as the production of by-product G) takes place:

$$\mathrm{C} \xrightarrow{r_2,\,\Delta H_2} \mathrm{F} + \mathrm{G},$$

with

$$\text{stoichiometric coefficients} \quad v_{\mathrm{C2}} = -1, v_{\mathrm{F2}} = -1, v_{\mathrm{F2}}, v_{\mathrm{G2}} = 1.$$

It is known that the conversion runs too quickly to perform a calorimetric investigation under isothermal conditions. Hence, the investigation must be carried out using the isoperibolic procedure.

To carry out the investigation, a batch of amino hydrochloride in the measuring kettle is brought to a reaction temperature of 50 °C and a pH-value of 0.7. To start the reaction, the stoichiometric amount of aqueous alkali nitrite at 50 °C is injected in a time interval of less than 2 s. Figure 5.17 shows the temporal course of the natural logarithm of the difference between the measured and the initial temperature $(T_2 - T_{20})$ after the start of injection. The reaction in the solution increases immediately upon dosing, achieves a maximum at the end of dosing and then decreases monotonously. The temperature decay slows down after about 10 s for a short time. Visual control of the process reveals the precipitation of solid matter. The brief slowing down of the temperature decay occurs obviously by the heat release due to the sudden, short-term precipitation in the already supersaturated reaction mixture. Then the subsequent precipitation takes place synchronously with the continuing conversion. The analysis of the solid matter shows that it is the desired heterocyclic product **F**.

For a comparison with the measured reaction curve, Fig. 5.17 presents in addition the curve of the temperature decay which is the result of a short-term heating up of the mixture following completion of the conversion by the electric heater to the maximum temperature $T_{2\mathrm{Max}}$ and then of its switch-off.

Elaboration of the thermokinetic data takes place according to

- The procedure of results of non-isothermal reactions (Sect. 4.2.3.1.1).
- The determination of the enthalpy of reaction, heat capacity and specific heat is given in Chap. 6.

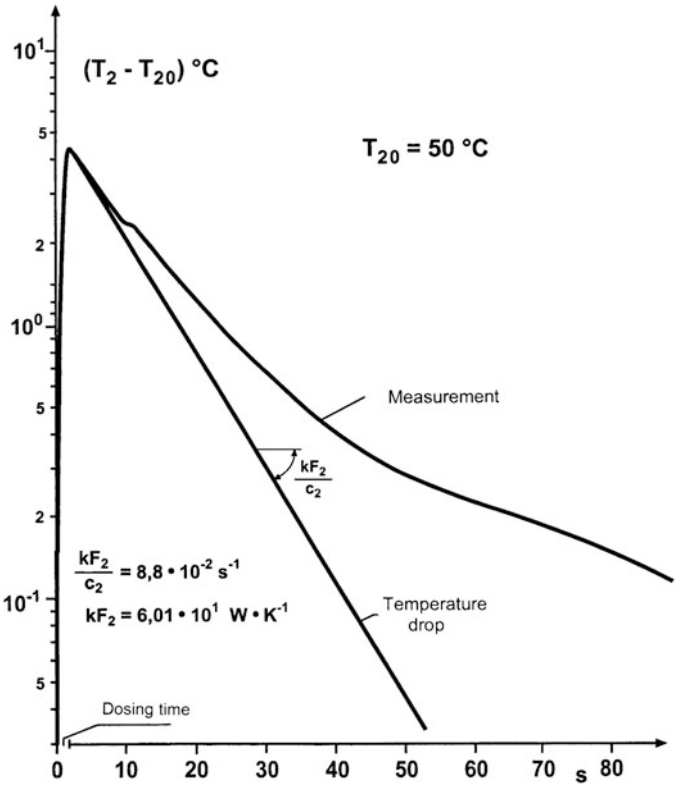

Fig. 5.17 Temporal course of difference between measured and initial temperature $(T_2 - T_{20})$ during heterocyclic reaction. Batch: 140 g aqueous solution of amine hydrochloride A. Dosage: 10 g aqueous solution of alkali nitrite B. Equal number of mol: 4.5×10^{-2}; pH = 0.7

The instant increase in temperature by the start of the dosage of alkali nitrite and the instant cessation at the end of dosing shows that the formation of the salt **C** occurs instantly; hence we have

$$r_2 = r_{\text{ring-closure}} \ll r_{\text{salt-formation}} = r_1 \cong \infty.$$

From the temperature difference $(T_{2\text{Max}} - T_{20})$, the effective heat capacity C_2 and the used number of mols N_0 amine hydrochloride yields the overall heat $(-\Delta H_{\lambda 1})$ of the formation of **C** (sum of the heat of physicochemical mixing and the heat of the desired reaction) according to[4]

[4] For determination of the effective heat capacity C_2 and the heat transfer coefficient $(k{\cdot}F)_2$ see Chap. 6.

$$-\Delta H_{\lambda 1} = C_2 \cdot (T_{2\mathrm{Max}} - T_{20})/N_0$$
$$= 87 \cdot (1 \pm 0.02)\ \mathrm{kJ/formula\ conversion.}$$

The sum of the heats of ring closure and of the accompanying precipitation $-(\Delta H_{\lambda 2} + \Delta H_{\lambda \mathrm{Pr}}) = \int_{t\ \mathrm{Dosing}\ \mathrm{end}\to\infty} q \cdot \mathrm{d}t/N_0$ results from the difference in the total amount of heat released $\int_{0\to\infty} (T_2 - T_{20}) \cdot \mathrm{d}t \cdot kF_2$ and the amount of heat released $(-\Delta H_{\lambda 1}) \cdot N_0$ by the formation of salt **C:**

$$-(\Delta H_{\lambda 2} + \Delta H_{\lambda \mathrm{Pr}}) = \int_{0\to\infty} (T_2 - T_{20}) \cdot \mathrm{d}t \cdot kF_2/N_0 - (-\Delta H_{\lambda 1})$$
$$= \int_{0\to\infty} (T_2 - T_{20}) \cdot \mathrm{d}t \cdot kF_2/N_0 - 87\ \mathrm{kJ/formula\ conversion}$$
$$= 39.3 \cdot (1 \pm 0.03)\ \mathrm{kJ/formula\ conversion.}$$

The temporal course of the total thermal reaction power $q = q_1 + q_2 + q_\mathrm{F}$ during the formation of ***C***, the ring closure and the accompanying precipitation results analogously in (2.14), i.e. from the data $(T_2 - T_\mathrm{S}), \mathrm{d}(T_2 - T_\mathrm{S})/\mathrm{d}t, q_{\mathrm{St}2}$ as well as $(k{\cdot}F)_2$ and C_2, respectively from the recorded data $(T_2 - T_{20}), \mathrm{d}(T_2 - T_{20})/\mathrm{d}t$ as well as $(k{\cdot}F)_2$ and C_2 because, due to the large degree of dilution, it can be assumed that $q_{\mathrm{St}2} = \mathrm{const}$, thus $q_{\mathrm{St}2} = (k \cdot F)_2 \cdot (T_{20} - T_\mathrm{S})$.[5]

For $t > t_{\mathrm{end\ of\ dosage}}$ we have $q_1(t) = 0$, hence $q = q_2 + q_\mathrm{F}$. By means of q, $(\Delta H_{\lambda 2} + \Delta H_{\lambda \mathrm{Pr}})$, (4.148) and (4.149) the auxiliaries $A(t)$ and $B(t)$ respectively y and x are calculated. Plotting y against x allows us to determine the rate order n of the ring closure and its activation energy E due to (4.154):

$$\ln\{A_1/A_2\}/\ln\{B_1/B_2\} = n - E/R \cdot [1/T_{21} - 1/T_{22}]/\ln\{B_1/B_2\}$$

or

$$y = n - E/R \cdot x.$$

Figure 5.18 shows plot y versus x. From the slope of the fitted curve results the activation temperature E/R, i.e.

$$E = 94.1\ \mathrm{kJ/mol.}$$

From its intersection with the ordinate we get

$$n = 0.9.$$

[5] With $q_\mathrm{Mi} = 0$: (2.16 and 2.25) $\equiv\ C_2 \cdot \mathrm{d}(T_2 - T_{20})/\mathrm{d}t = q - (k \cdot F)_2 \cdot (T_2 - T_{20})$.

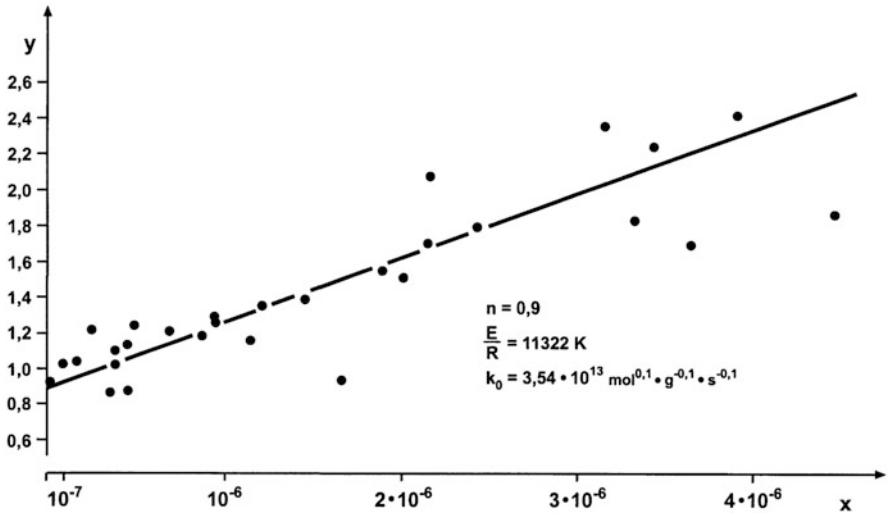

Fig. 5.18 Plot $Y = n - E/R \cdot X$ and fitted curve

The recorded data $T_2(t)$, $A(t)$ and $B(t)$ give, due to (4.155), the rate coefficients $k(T_{2(t)})$, for instance $k_2\left(T_{2(t=25\ \mathrm{s})}\right) = k_2(51\ ^\circ\mathrm{C}) = 2.36\ \mathrm{mol}^{0.1}\ \mathrm{g}^{-0.1}\ \mathrm{s}^{-1}$, and from that, according to the Arrhenius relation, we get the pre-exponential factor

$$ko_2 = 3.54 \times 10^{13}\ \mathrm{mol}^{0.1}\ \mathrm{g}^{-0.1}\ \mathrm{s}^{-1}.$$

Hence, the overall rate function of the ring closure reads

$$r = k_2 \cdot c_\mathrm{C}^n = ko_2 \cdot \mathrm{EXP}(-94,100/R \cdot T) \cdot c_\mathrm{C}^{0.9}.$$

5.2.2 *Reaction of a Substituted Triazine with a Substituted Naphthylamine Sulphonic Acid in Water*

An example of the working out of the kinetics of a very quick reaction

- From the data of non-isothermal, discontinuous runs
- On the basis of mathematical-analytical relations

the irreversible reaction of a substituted triazine A and a substituted naphthylamine sulphonic acid B in aqueous solution is discussed. The reaction system is

$$\mathrm{A} + \mathrm{B} \xrightarrow[(\mathrm{H_2O})]{r_1,\ \Delta H_1} \mathrm{C} + \mathrm{D},$$

with

$$\text{stoichiometric coefficients } \nu_{A1} = -1, \nu_{B1} = -1, \nu_{C1} = 1, \nu_{D1} = 1.$$

Triazine reacts also with water. Hence, besides the desired conversion, the following parasitic reaction runs:

$$A + H_2O \overset{r_1, \Delta H_1}{\underset{(H_2O)}{\rightarrow}} F + D,$$

with

$$\text{stoichiometric coefficients } \nu_{A2} = -1, \nu_{H2O2} = -1, \nu_{F2} = 1, \nu_{D2} = 1.$$

It is known that the conversion runs very quickly, but it is unknown whether the reaction runs within the time interval of a minute or only of some seconds. This knowledge is important for technical production with regard to both chemical engineering and security. In addition, the enthalpy of reaction is unknown and therefore must be measured.

The investigation is carried out under isoperibolic conditions as follows.

- The batch in the measuring kettle consists of an aqueous solution of naphthylamine sulphonic acid **B** or pure water.
- The batch is brought to the temperature of reaction T_0.
- Triazine **A** at temperature T_0 is instantly injected (duration of injection $\ll 1$ s) to start the conversion.
- The course of the temperature versus time is recorded.

Figure 5.19 gives an example of a characteristic run of the temperature. The soon-to-appeare temperature maximum after the injection of A confirms the unusual speed of the conversion. The course of the distorted signal of the temperature by the sensor must be antidistorted, i.e. (2.22) and (2.24) must be applied to make it possible for a kinetic interpretation to be done.

The desired reaction and the parasitic reaction are coupled parallel reactions. It is assumed in a first assumption that both reactions run according to a rate function of order 1 with respect to A. Hence, due to (4.44), for the thermal reaction power we get

$$q(t) = k \cdot c_{A0} \cdot V \cdot (-\Delta H_\lambda) \cdot \mathrm{EXP}[-k \cdot t], \tag{5.23}$$

with $k = \left(\overline{k_1 + k_2}\right)_{T_{start} \rightarrow T_{max}}$ because of the relatively small temperature increase.

The combination of (2.24) and (5.23) gives as a result the rate of change in the real temperature T_2 in the reaction mixture:

$$\mathrm{d}(T_2 - T_{20})/\mathrm{d}t \; = \; a \cdot \mathrm{EXP}[-k \cdot t] \; - \; b \cdot (T_2 - T_{20}), \tag{5.24}$$

with

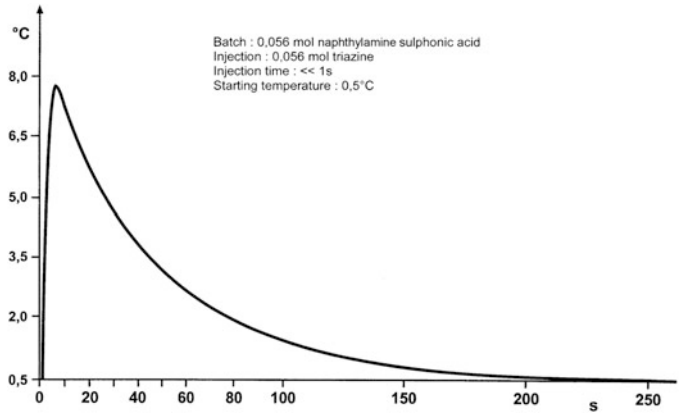

Fig. 5.19 Temporal course of signal T_{2F} of temperature sensor after injection of triazine A in aqueous solution of naphthylamine sulphonic acid B, non-isothermal, isoperibolic, discontinuous reaction

$$a = k \cdot c_{A0} \cdot V \cdot (-\Delta H_\lambda)/C_2, b = kF_2/C_2.$$

The solution of (5.24) is

$$T_2 = a/(k-b) \cdot \{\mathrm{EXP}[-b \cdot t] - \mathrm{EXP}[-k \cdot t]\} + T_{20}. \tag{5.25}$$

Substitution of (5.25) into (2.22) and solving the equation gives as a result the equation for the temporal course of the signal T_F by the temperature sensor:

$$\begin{aligned} T_F = {} & \beta \cdot a/(k-b) \cdot \{\mathrm{EXP}[-b \cdot t]/(\beta - b) - \mathrm{EXP}[-k \cdot t]/(\beta - k) \\ & -\{1/(\beta - b) - 1/(\beta - k)\} \cdot \mathrm{EXP}[-\beta \cdot t]\} + T_{20} \end{aligned} \tag{5.26}$$

T_F passes a maximum value at the time t_{Fmax}, where the differentiation of T_F equals zero,

$$\begin{aligned} 0 = {} & (\beta - b)/(\beta - k) \cdot \{k \cdot \mathrm{EXP}[-k \cdot t_{Fmax}] - \beta \cdot \mathrm{EXP}[-\beta \cdot t_{Fmax}]\} + \beta \\ & \cdot \mathrm{EXP}[-\beta \cdot t_{Fmax}] - b \cdot \mathrm{EXP}[-b \cdot t_{Fmax}]. \end{aligned} \tag{5.27}$$

This relation is used for the evaluation of the rate coefficient k, for instance by means of the conventional zero-position method.

Knowledge of the necessary quantity of b and β arises in the following way. By the injection of a small amount of reacted mixture (taken beforehand from the reacted mixture and brought to a temperature $T > T_{20}$) in the reacted mixture, the temperature T_{20} jumps quasi-instantly to the temperature T_{2M} and then decreases due to heat outflow to achieve T_{20} again (Fig. 5.20).

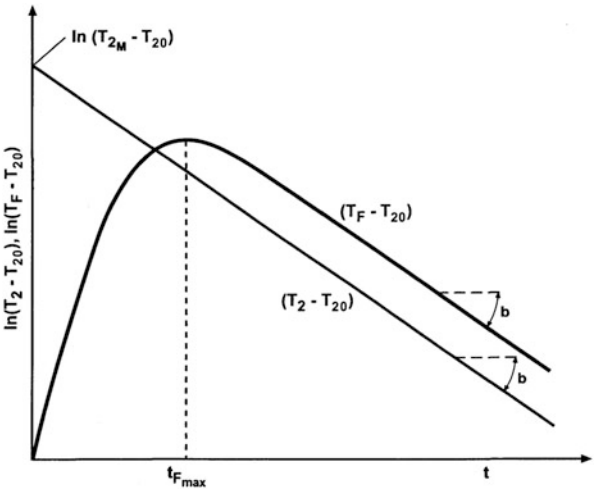

Fig. 5.20 Temporal course of difference
• $T_2 - T_{20}$ of real temperature T_2 in reacted mixture after abrupt temperature jump from $T_2 = T_{20}$ to $T_2 = T_{2M}$ at time $t = 0$ by injection of reacted mass
• $T_F - T_{20}$ of signal T_F of temperature sensor, non-isothermal, isoperibolic, discontinuous reaction

The solution of (2.24) gives, according to the present conditions, the temporal course of the real temperature decay in the reaction mixture:

$$T_2 = (T_{2M} - T_{20}) \cdot \mathrm{EXP}(-b \cdot t) + T_{20}. \tag{5.28}$$

Combining (5.28) and (2.22) and solving the resulting differential equation gives as a result the course of the temperature signal of the sensor:

$$T_F = \beta \cdot (T_{2M} - T_{20})/(\beta - b) \cdot (\mathrm{EXP}[-b \cdot t] - \mathrm{EXP}[-\beta \cdot t]) + T_{20}\,. \tag{5.29}$$

The sensor signal reaches its maximum at the time t_{Fmax} and then decreases monotonously to T_{20}. Because $\beta \gg b$, the logarithmic plot of T_F versus time turns for $t \gg 0$ into a straight line, where

$$\kappa = b.$$

Differentiating (5.29), setting to zero and rearranging results in

$$t_{Fmax} = \ln\{\beta/b\}/(\beta - b).$$

From that follows β, for instance using the conventional zero-position method.

By means of (5.27), from experiments with different $A_0 = B_0$ the average overall rate results:

$$k = 1.52 \times (1 \pm 0.27)\ \mathrm{s}^{-1}.$$

Some conversions of pure water and triazine A give an average rate coefficient of the parasitic parallel reaction:

$$k_2 = 0.11 \times (1 \pm 0.3)\ \ \mathrm{s}^{-1}.$$

Thus, according to (4.41), the rate coefficient of the desired reaction is

$$k_1 = 1.41 \times (1 \pm 0.27)\ \ \mathrm{s}^{-1}.$$

Hence, the parasitic reaction runs approximately 13 times slower than the desired one.

The value of the overall heat of reaction is determined[6]:

$$(-\Delta H_\lambda) = 135 \times (1 \pm 0.15)\ \ \mathrm{kJ/formula\ \ conversion}.$$

The heat of the parasitic reaction results by means of the injection of triazine in pure water:

$$(-\Delta H_{\lambda 2}) = 341 \times (1 \pm 0.08)\ \ \mathrm{kJ/formula\ \ conversion}.$$

Corresponding to (4.45), the heat of reaction of the desired conversion can be calculated by means of $k,\ k_1,\ k_2, (-\Delta H_\lambda)$ and $(-\Delta H_{\lambda 2})$. We obtain

$$(-\Delta H_{\lambda 1}) = 119 \times (1 \pm 0.15)\ \ \mathrm{kJ/formula\ \ conversion}.$$

Figure 5.21 presents a calculated and measured T-curve.

The conformance of experiment with calculation is sufficient in view of the fact that

- For simplification the temperature dependency of the rate coefficient is not correctly considered (Arrhenius equation).
- Instead, a rate coefficient averaged over the temperature interval is used.
- Only the reaction time t_{Rt} needs to be estimated for a quasi-complete conversion.

The rule of thumb for the determination of the reaction time t_{Rt} reads for a rate of order 1

Reaction time for quasi-complete conversion $t_{\mathrm{Rt}} \cong 6 \cdot$ half-life $\iota_{1/2}$.

This yields in the case at hand

$$t_{\mathrm{Rt}} \cong 6 \cdot \iota_{1/2} = 6 \cdot \ln\{2\}/k = 2.74\ \ \mathrm{s}.$$

Hence, after approximately 3 to 4 s the reaction is practically finished.

When the desired and parasitic reactions run according to a rate function of order 2, the thermal reaction power is due to (4.51):

[6] See Sect. 6.1.2.

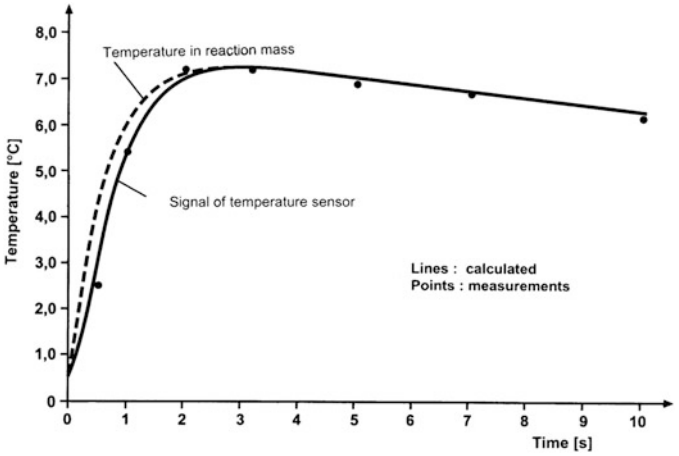

Fig. 5.21 Conversion of triazine A and naphthylamine sulphonic acid B in aqueous solution:
$A + B \rightarrow C + D$
$A + H_2O \rightarrow F + D$
$r_1 = k_1 * c_A, r_2 = k_2 * c_A$
$A0 = B0 = 0.056\,\text{mol}$, $T_0 = 0.5\ ^\circ\text{C}$
Rate coefficient $k = \overline{(k_1 + k_2)}_{T\text{start}\rightarrow T\text{max}} = 1.31/\text{s}$, $\beta = 5.522/\text{s}$, $b = 2.255 \times 10^{-2}/\text{s}$
Overall reaction heat$(-\Delta H_\lambda) = 135$ kJ/formula conversion, $C_2 = 1,050$ J/K
non-isothermal, polytropic, discontinuous reaction

$$q(t) = {c_{A0}}^2 \cdot (k_1 + k_2) \cdot V \cdot (-\Delta H_\lambda)/[c_{A0} \cdot (k_1 + k_2) \cdot t \cdot 1]^2 \tag{5.30}$$

From the combination of (2.24) and (5.29) we obtain the change rate in the temperature T_2 of the reaction mixture:

$$\mathrm{d}(T_2 - T_{20})/\mathrm{d}t = \mathrm{e}/(\mathrm{d} \cdot t + 1)^2 - b \cdot (T_2 - T_{20}),$$

with

$$\begin{aligned} \overline{(k_1 + k_2)}_{T\text{start}\rightarrow T\text{max}} = k,\ d = c_{A0} \cdot k,\ e = {c_{A0}}^2 \cdot k \cdot V \cdot (-\Delta H_\lambda)/C_2, \\ b = (k \cdot F)_2/C_2. \end{aligned} \tag{5.31}$$

When in contrast against that the parasitic reaction runs according to a rate function of order 1 (for instance, due to the large excess of water) the thermal reaction power is, according to (4.46), with $э = 2 \cdot k_2/k_1$,

$$\begin{aligned} q = \Big[& k_1 \cdot (-\Delta H_1) \cdot V/\left\{\left({c_{A0}}^{-1} + э\right) \cdot \mathrm{EXP}(k_1 \cdot t) - э\right\}^2 \\ & + k_2 \cdot (-\Delta H_2) \cdot V/\left\{\left({c_{A0}}^{-1} + э\right) \cdot \mathrm{EXP}(k_1 \cdot t) - э\right\}\Big]. \end{aligned} \tag{5.32}$$

The combination of (2.24) and (5.32) gives the change rate in temperature T_2:

$$\mathrm{d}(T_2 - T_{20})/\mathrm{d}t = \left[k_1 \cdot d_1/\{e \cdot \mathrm{EXP}(k_1 \cdot t) - \ni\}^2 + k_2 \cdot d_2/\{e \cdot \mathrm{EXP}(k_1 \cdot t) - \ni\}\right] - b \cdot (T_2 - T_{20}), \tag{5.33}$$

with

$$\overline{(k_1)_{T\mathrm{start}\to T\max}} = k_1,\ \overline{(k_2)_{T\mathrm{start}\to T\max}} = k_2,\ d_1 = (-\Delta H_1) \cdot V/C_2,\ d_2 = (-\Delta H_2) \cdot V/C_2,\ e = c_{\mathrm{A}0}^{-1} + \ni,\ b = k \cdot F_2/C_2.$$

Analytical solutions of Eqs. (5.31) and (5.33) in the explicit form $T_2 = f(t)$ respectively of the combination of (5.31) and (5.33) with (2.22) in the explicit form $T_{2\mathrm{F}}(t)$, i.e. the signals of the temperature sensor, do not exist. Only numerical solutions of the equations are possible. Hence, the working-out procedure for k_i consists in numerical fitting of the measured curves of $T_{2\mathrm{F}}$.

Figure 5.22 shows for example a comparison of the measured and computed temperature signal $T_{2\mathrm{F}}$ on the assumption of the following rate functions:

(a) Both the desired and parasitic reaction of order 1
(b) Desired and parasitic reaction of order 2
(c) Desired reaction of order 2 and parasitic reaction of order 1

The best fit gives the assumption of order 1 for both reactions.

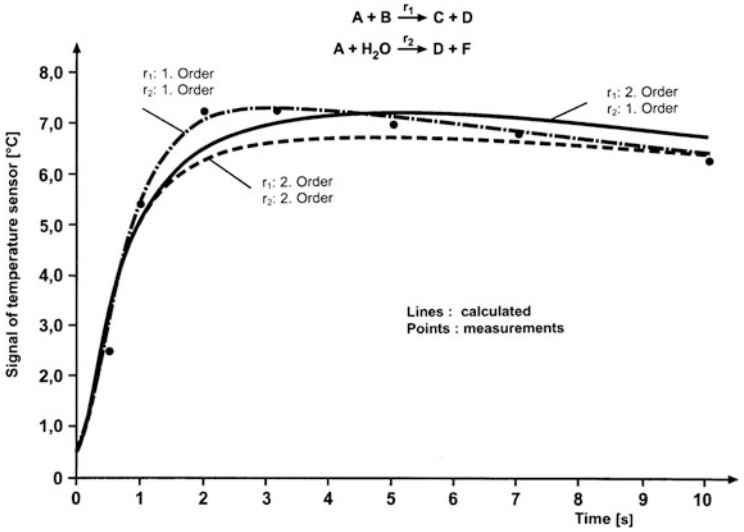

Fig. 5.22 Comparison of sensor signal $T_{2\mathrm{F}}$ versus time for different rate orders of conversion, triazine A and naphthylamine sulphonic acid B, in aqueous solution, non-isothermal, discontinuous reaction, isoperibolic condition, $\mathrm{A}_0 = \mathrm{B}_0$

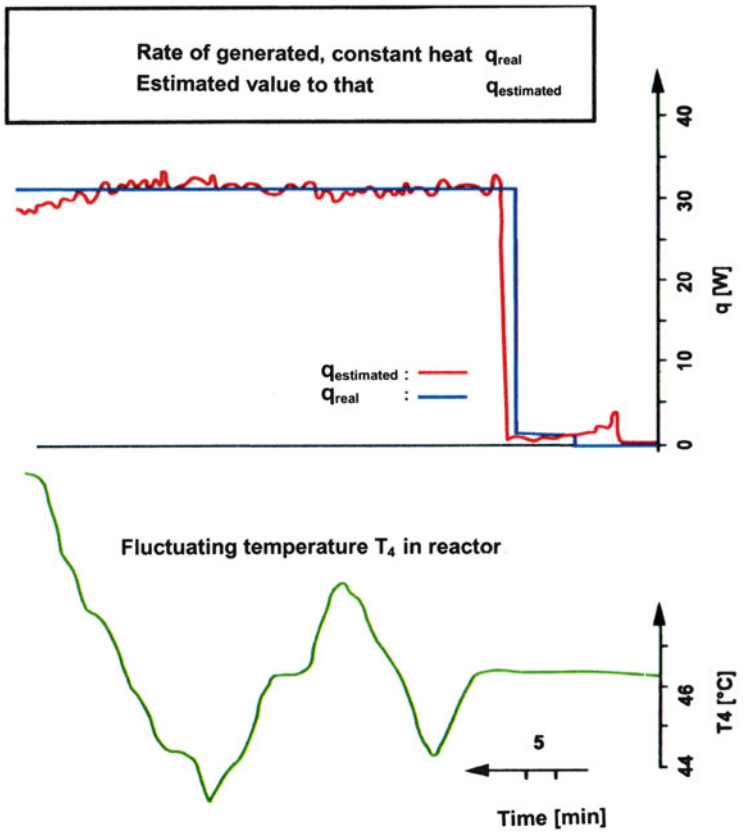

Fig. 5.23 Test of functionality of the sensor. Constant electric heating power q_{real} and its online estimated value $q_{estimated}$. The temperature T in the virtual tank reactor alternates

5.3 Measurements of Online Calorimeter (Sensor)

The run of a reaction is simulated to ensure the functionality of the online calorimeter. To that end the measuring kettle is

- Supplied with an additional electric heater of the same design as described in Sect. 2.1.1;
- Placed in the external circulation of a thermostat, which is filled with silicone oil.

An induced change in temperature in the thermostat simulates the temperature fluctuations T_4 within the technical tank reactor; the working heater in the measuring kettle simulates the thermal reaction power within the tank reactor.

The heater works initially at a constant rate of heat release q while the temperature T_4 of the thermostat (virtual tank reactor) fluctuates (Fig. 5.23).

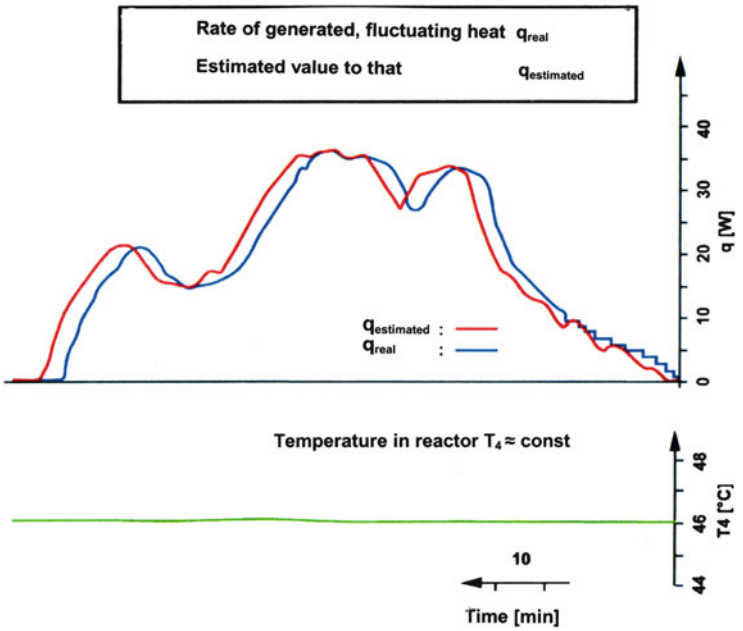

Fig. 5.24 Test of functionality of the sensor. Constant electric heating power q_{real} and its online estimated value $q_{\text{estimated}}$. The temperature T in the virtual tank reactor alternates

The illustration shows the conformity of the actual rate of heat release to the estimated one. The estimated line appears with a time lag of approximately 3 min due to the chosen finite estimation time of the Kalman–Bucy filter.

Figures 5.24 and 5.25 show the courses of a fluctuating electric heating power q and their estimated courses for a

- Constant
- Induced fluctuating

temperature T_4 of the thermostat (virtual tank reactor).

To measure the thermal reaction power q of a real reaction, the online calorimeter is placed in the circulation of an ideally mixed batch reactor with 15 L volume. In the batch reactor is installed an electric heater of the same design as described in Sect. 2.1.1.

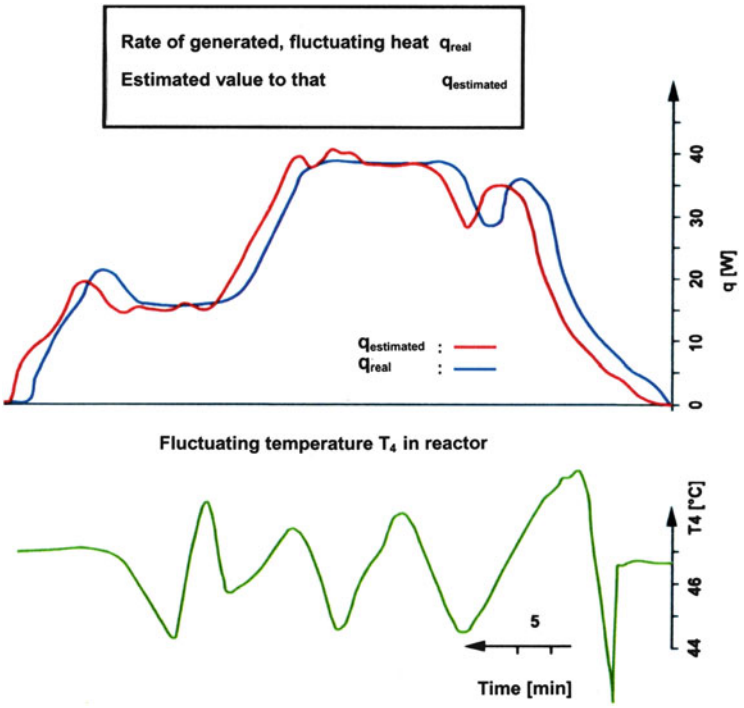

Fig. 5.25 Test of functionality of the sensor. Constant electric heating power q_{real} and its online estimated value $q_{\text{estimated}}$. The temperature T in the virtual tank reactor alternates

The reaction is the alcoholysis of acetic acid anhydride by methanol. Pyridine catalyses the conversion. For the start of the reaction, methanol is dosed as quickly as possible in a batch of acetic anhydride, which is mixed with some added acetic acid as acting accelerator for solving. By the injection of pyridine at an advanced state of conversion, the reaction velocity is once more abruptly enlarged. Then the conversion ends in a relatively short amount of time. The temperature fluctuations in the batch reactor are induced during the conversion by means of the installed electric heater. Figure 5.26 shows the courses of thermal reaction power q and the accompanying induced change in temperature within the batch reactor.

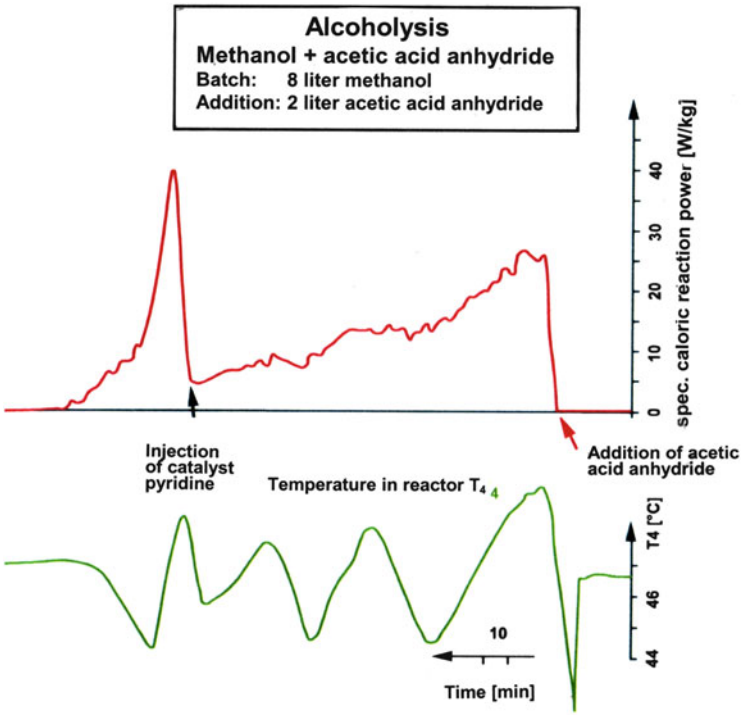

Fig. 5.26 Online measurement of the thermal reaction power q by the sensor during the reaction of methanol and acetic acid anhydride in a tank reactor. The alternating temperature in the reactor is induced